ACR No. 3H28

NATIONAL ADVISORY COMMITTEE FOR AERONAUTICS

WARTIME REPORT

ORIGINALLY ISSUED
August 1943 as
Advance Confidential Report 3H28

WIND-TUNNEL TESTS OF AILERONS AT VARIOUS SPEEDS

IV - AILERONS OF 0.20 AIRFOIL CHORD AND TRUE CONTOUR WITH 0.35 AILERON-CHORD EXTREME BLUNT-NOSE BALANCE ON THE NACA 23012 AIRFOIL

By W. Letko, T. A. Hollingworth, and R. A. Anderson

Langley Memorial Aeronautical Laboratory
Langley Field, Va.

NACA

WASHINGTON

L - 433

NATIONAL ADVISORY COMMITTEE FOR AERONAUTICS

ADVANCE CONFIDENTIAL REPORT

WIND-TUNNEL TESTS OF AILERONS AT VARIOUS SPEEDS

IV - AILERONS OF 0.20 AIRFOIL CHORD AND TRUE CONTOUR WITH 0.35 AILERON-CHORD EXTREME BLUNT-NOSE BALANCE ON THE NACA 23012 AIRFOIL

By W. Letko, T. A. Hollingworth, and R. A. Anderson

SUMMARY

Tests were made on an NACA 23012 airfoil fitted with a 20-percent-chord, true-contour aileron with 35-percent-chord, extreme blunt-nose balance. The tests were made in the two-dimensional test section of the NACA stability tunnel at a range of airspeeds from 160 to 360 miles per hour, which corresponded to a range of Mach numbers from 0.195 to 0.475. The primary purpose of the investigation was to determine the variation of the aerodynamic characteristics of this type of aileron with airspeed; the effect of variations of gap width and balance-nose radii was also investigated.

The results of the investigation are presented as curves of section hinge-moment coefficient and section lift coefficient plotted against aileron angle, and cross plots have been made to illustrate the effect of variations of Mach number, balance-nose radii, and gap width on the aerodynamic characteristics of the aileron. For small aileron deflections at low angles of attack, increased airspeed had little effect on the rate of change of section hinge-moment coefficient with aileron deflection but increased the rate of change of section lift coefficient with aileron deflection. Increased airspeed decreased the unstalled range of the aileron and increased the rate of change of section lift coefficient and section pitching moment coefficient with angle of attack. An increase in gap width at low angles of attack for small aileron deflections decreased the rate of change of section lift coefficient with aileron deflection and appreciably decreased the rate of change of section hinge-moment coefficient with

aileron deflection. Increased balance-nose radii increased the rate of change of section hinge-moment coefficient with aileron deflection for small aileron deflections and appreciably increased the unstalled range of the aileron.

INTRODUCTION

The recent trend in airplane design toward increased size, power, and radius of gyration in roll and the demand for greater maneuverability at high airspeeds have made necessary almost perfectly balanced controls on combat aircraft with no decrease in control effectiveness. Although most present aileron installations are fairly satisfactory at low airspeeds, these installations may be unsatisfactory at high airspeeds because of insufficient balance and, in some cases, overbalance. In an effort to overcome this difficulty, the NACA has undertaken a series of investigations to determine the aerodynamic characteristics of various types of balanced control surfaces at higher airspeeds than were used in their development. The results of similar tests have been reported in references 1, 2, and 3.

The present report contains the results of tests of a 20-percent-chord aileron with a 35-percent-chord extreme blunt nose balance on an NACA 23012 airfoil; the aileron was similar to that of reference 1 with the exception of the airfoil section contour. A 0.35-aileron-chord balance was chosen because the results of reference 4 obtained at low airspeeds indicated that this aileron would give almost comlete balance at a low angle of attack.

The section lift and hinge-moment coefficients were measured for various values of balance-nose radii and gap widths at airspeeds up to 360 miles per hour over a range of aileron deflections of ±20° and a range of angle of attack from -5° to 10°. The results of the investigation are presented as curves of section hinge-moment coefficient and section lift coefficient plotted against aileron angle. Cross plots have been made to show the effect of variations of gap width, balance-nose radii, and airspeed on the aerodynamic characteristics of the aileron.

SYMBOLS

c_l airfoil section lift coefficient (l/qc)

c_{h_a} aileron section hinge-moment coefficient $(h_a/q\, c_a{}^2)$

$c_{m_{c/4}}$ airfoil section pitching-moment coefficient about the quarter-chord point of airfoil $\left(\frac{m_{c/4}}{q\ c^2}\right)$

l airfoil section lift

h_a aileron section hinge moment

c chord of basic airfoil, including aileron

c_a chord of aileron measured from hinge axis back to trailing edge

q dynamic pressure $\left(\frac{1}{2}\rho V^2\right)$

V air velocity

ρ mass density of air

$m_{c/4}$ airfoil section pitching moment about the quarter-chord point of the airfoil

α_o angle of attack for airfoil of infinite aspect ratio

δ_a aileron angle with respect to airfoil

M Mach number

$\left(\frac{\partial c_{h_a}}{\partial \delta_a}\right)_{\alpha_o}$ slope of c_{h_a} against δ_a at constant α_o obtained from the faired curve of c_{h_a} against δ_a at -5° and 5° aileron deflections

$\left(\frac{\partial c_{h_a}}{\partial \alpha_o}\right)_{\delta_a}$ slope of c_{h_a} against α_o at constant δ_a

$\left(\frac{\partial c_l}{\partial \alpha_o}\right)_{\delta_a}$ slope of c_l against α_o at constant δ_a

$\left(\frac{\partial c_l}{\partial \delta_a}\right)_{\alpha_o}$ slope of c_l atainst δ_a at constant α_o obtained from the faired curve of c_l against δ_a at -5° and 5° aileron deflections

APPARATUS AND MODEL

The tests on the NACA 23012 airfoil equipped with an extreme blunt-nose balance aileron were made in the rectangular 2.5- by 6-foot test section of the stability tunnel. The model completely spanned the test section and was fixed into end disks that were flush with the sides of the tunnel. The end disks were rotated to change the angle of attack. A photograph of the airfoil mounted in the tunnel is shown in figure 1. Figure 2 is a sketch showing the aileron configurations tested.

The airfoil was made principally of laminated mahogany. The aileron, with the exception of a wooden leading edge, was made of steel and rotated in ball bearings. These bearings were set into steel end plates mounted on the ends of the airfoil. A full-span seal of impregnated cotton fabric was used for the tests with the gap sealed. The aileron angle and hinge moment were measured by a calibrated spring-torque balance and sector system. The airfoil lift was measured by an integrating manometer connected to orifices set in the floor and ceiling on the center line of the tunnel. The integrating manometer was calibrated from pressure-distribution data. The pressure distribution was recorded photographically from a multiple manometer connected to pressure orifices located on the midspan of the wing and aileron.

TESTS

Section hinge-moment and section lift coefficients were measured at five airspeeds corresponding to a range of Mach numbers from 0.195 to 0.475. These test airspeeds corresponded to Reynolds numbers, based on a 2-foot chord and standard atmosphere, of approximately 2,800,000 to 6,700,000, respectively. Figure 3 shows the variation of different test Mach numbers with approximate Reynolds numbers. At each airspeed, tests were run at angles of attack of -5°, 0°, 5°, and 10°. For each angle of attack, gap widths of 0.0005c, 0.0030c, 0.0055c (sealed and unsealed) and 0.0107c were tested with balance-nose radii of 0, 0.01c, and 0.02c. (See fig. 2.) The integrating manometer results are not available for the zero nose radius. For each of the conditions, tests were made with aileron angles of 0°, $\pm5^\circ$, $\pm7^\circ$, $\pm10^\circ$, $\pm13^\circ$, $\pm16^\circ$, $\pm18^\circ$, and $\pm20^\circ$. At high angles of attack and high aileron deflections, however, power was not available to obtain the highest speeds.

At each angle of attack, photographic records of pressure distribution were taken at aileron angles of 0°, ±5°, ±10°, and ±16° for Mach numbers of 0.195, 0.358, and 0.455.

PRECISION

The aileron angle and angle of attack were set to within ±0.3° and ±0.1°, respectively. The aileron section hinge-moment coefficients could be repeated to within ±0.003 and the lift coefficients to within ±0.01. Lift and pitching-moment coefficients and angle of attack were corrected for tunnel-wall effect by the following formulas:

$$c_l = \left[1 - Y\,(1 + 2\beta)\right] c_l'$$

$$\alpha_o = (1 + Y)\,\alpha_o'$$

$$c_{m_{c/4}} = (1 - 2\beta Y)\,c_{m_{c/4}}' + \frac{Y c_l'}{4}$$

where

$$Y = \frac{\pi^2}{48}\left(\frac{c}{h}\right)^2$$

c airfoil chord (2 ft)

h height of tunnel (6 ft)

$\beta = 0.237$ (theoretical factor for NACA 23012 airfoil)

c_l' measured lift coefficient

α_o' uncorrected or geometric angle of attack

$c_{m_{c/4}}'$ measured pitching-moment coefficient

The values used are:

$$c_l = 0.966c_l'$$

$$\alpha_o = 1.023\alpha_o'$$

$$c_{m_{c/4}} = 0.989c_{m_{c/4}}' + 0.006c_l'$$

The hinge moments were not corrected for tunnel-wall effect but were measured both by pressure distribution and by the spring-torque balance for a number of conditions; a comparison of the results of the two methods is given in figure 4. The variations shown are probably due to the fact that the spring-torque balance measures the moment of the entire aileron, which includes the effects of boundary layer at the tunnel wall and of gaps at the ends of the aileron as well as any cross flow over the aileron. The pressure distribution, however, gives the hinge moment of one section of the aileron and is subject to errors in fairing the pressure-distribution curves. The effect of compressibility on these corrections has been neglected; it is believed, however, that the conclusions given in the present report are not invalidated.

RESULTS AND DISCUSSION

In order that the results for the tests may be more easily found, the figure numbers, the variations shown on the figure, and the corresponding model configurations are given in table I.

Hinge Moments

Curves of section hinge-moment coefficient c_{h_a} plotted against aileron deflection δ_a are presented in figures 5 to 10. The results, in general, indicate that good balance effectiveness was maintained for a limited range of aileron angles; for large aileron angles, separation of flow caused rapid increases in the hinge-moment coefficients.

In the unstalled range of aileron angles, the slopes of the curves of c_{h_a} against δ_a were small and generally negative for positive aileron deflections at negative angles of attack and increased negatively with an increase in angle of attack. In most cases, the slopes of the curves changed in the vicinity of the neutral aileron setting and at negative aileron angles were smaller than at positive angles for all angles of attack except at $\alpha_o = -5^\circ$, at which the negative slope was fairly large.

An oscillation frequently occurred during the tests at the transition point between the stalled and unstalled range. The amplitude of this oscillation increased with airspeed. The principal effect of increased airspeed, however, was an appreciable decrease in the unstalled range of the aileron. (See figs. 5 to 10). This effect is probably due to the effects of both Reynolds number and Mach number. A comparison of the various test Mach numbers with the approximate Reynolds numbers is given in figure 3.

The effect of Mach number on $\left(\frac{\partial c_{h_a}}{\partial \delta_a}\right)_{\alpha_o}$ is shown in figures 11 to 14. At $\alpha_o = 0^\circ$ for all Mach numbers and $\alpha_o = \pm 5^\circ$ for low Mach numbers, the change in $\left(\frac{\partial c_{h_a}}{\partial \delta_a}\right)_{\alpha_o}$ with Mach number was nearly zero. At $\alpha_o = \pm 5^\circ$ for values of Mach number above about 0.4 and at $\alpha_o = 10^\circ$ for the range of Mach numbers tested, the value of $\left(\frac{\partial c_{h_a}}{\partial \delta_a}\right)_{\alpha_o}$ increased rapidly in the negative direction with Mach number. The increase in $\left(\frac{\partial c_{h_a}}{\partial \delta_a}\right)_{\alpha_o}$, which was probably caused by compressibility effects, appeared to occur at consistently higher Mach numbers with a sealed gap than with an open gap.

For the condition of high speed and $\alpha_o = 0^\circ$ with 0.02c balance-nose radii, values of $\left(\frac{\partial c_{h_a}}{\partial \delta_a}\right)_{\alpha_o}$ of −0.0008 for a gap of 0.0055c (fig. 11) and −0.0022 for the sealed gap (fig. 12) were obtained from this investigation as contrasted to values of −0.0075 and −0.0057, respectively, which are reported in reference 1 for a 66,2-216, a = 1 airfoil for the same conditions. This difference in the results indicates that the amount of balance required depends on the hinge moment of the unbalanced aileron. The hinge moment of the unbalanced aileron in turn depends on the shape of the airfoil section, particularly near the trailing edge. (See reference 8.)

An increase in the gap width tended to decrease slightly the unstalled range of the aileron; the effect was negligible, however, for most conditions (figs. 6 to 10). The effect of gap width on $\left(\frac{\partial c_{h_a}}{\partial \delta_a}\right)_{\alpha_o}$ is shown in figure 13. The change in $\left(\frac{\partial c_{h_a}}{\partial \delta_a}\right)_{\alpha_o}$ with gap width varied considorably with α_o. At $\alpha_o = 0^\circ$, increased gap width resulted in a decreased negative value of $\left(\frac{\partial c_{h_a}}{\partial \delta_a}\right)_{\alpha_o}$ at all airspeeds; this trend was also found in reference 4. At $\alpha_o = 10^\circ$, the manner in which $\left(\frac{\partial c_{h_a}}{\partial \delta_a}\right)_{\alpha_o}$ varied with gap width was dependent upon airspeed. At $M = 0.199$, the effect of gap width on $\left(\frac{\partial c_{h_a}}{\partial \delta_a}\right)_{\alpha_o}$ was negligible; whereas at $M = 0.417$, the values of $\left(\frac{\partial c_{h_a}}{\partial \delta_a}\right)_{\alpha_o}$ increased negatively with gap width up to a maximum negative value at a gap width of approximately 0.006c. For gap widths larger than 0.006c the negative values of $\left(\frac{\partial c_{h_a}}{\partial \delta_a}\right)_{\alpha_o}$ decreased. The values of $\left(\frac{\partial c_{h_a}}{\partial \delta_a}\right)_{\alpha_o}$ for the sealed gap corresponded closely to the values of the smallest gap widths for all conditions. A value of −0.0002 for $\left(\frac{\partial c_{h_a}}{\partial \delta_a}\right)_{\alpha_o}$ was indicated at $\alpha_o = 0^\circ$ when the gap width was

0.01c. An approximate value of $\left(\frac{\partial c_{h_a}}{\partial \delta_a}\right)_{\alpha_o}$ of −0.0072 was obtained for a plain sealed aileron in reference 5.

Increasing the balance-nose radii increased greatly the unstalled range of aileron angles, as shown in figures 5 and 6. Because the data for zero radii were incomplete and because the results for ailerons with small balance-nose radii (especially zero) showed that the stall occurred at such a small deflection that these ailerons have doubtful practical application, no curve for zero radii and only one for 0.01c radii is presented. The effect of balance-nose radii on $\left(\frac{\partial c_{h_a}}{\partial \delta_a}\right)_{\alpha_o}$ is shown in figure 14. In general, the value of $\left(\frac{\partial c_{h_a}}{\partial \delta_a}\right)_{\alpha_o}$ increased negatively with increased radii in the unstalled range, as was indicated in reference 4. An exception was found in the condition of the unsealed gap at low airspeeds where the value of $\left(\frac{\partial c_{h_a}}{\partial \delta_a}\right)_{\alpha_o}$ remained practically constant. In the unstalled range the rate of change of $\left(\frac{\partial c_{h_a}}{\partial \delta_a}\right)_{\alpha_o}$ with balance-nose radii was greatest with the gap sealed. (See fig. 14.) At $\alpha_o = 0^{\circ}$ and with the gap sealed, the aileron with balance-nose radii of zero was slightly overbalanced at all airspeeds.

Closely balanced ailerons may be overbalanced while rolling, depending on the value of $\left(\frac{\partial c_{h_a}}{\partial \alpha_o}\right)_{\delta_a}$. The variation of c_{h_a} with α_o at high and low Mach numbers for the open and the sealed gap is presented in figures 15 and 16, respectively. When $\delta_a = \pm 13^{\circ}$ the value of $\left(\frac{\partial c_{h_a}}{\partial \alpha_o}\right)_{\delta_a}$ is negative. With the aileron neutral, the value of $\left(\frac{\partial c_{h_a}}{\partial \alpha_o}\right)_{\delta_a}$ is positive at negative angles of attack and becomes negative with an increase in angle of attack. In general, the effect of gap width or of a variation in airspeed on $\left(\frac{\partial c_{h_a}}{\partial \alpha_o}\right)_{\delta_a}$ appears to be slight. The results of this investigation indicate that for large aileron angles, a reduction in stick force would be obtained while the airplane is rolling; the amount of reduction depends on the value of $\left(\frac{\partial c_{h_a}}{\partial \alpha_o}\right)_{\delta_a}$. Although the curve of c_{h_a} against α_o sometimes has a slight positive slope, there is little chance of overbalance for this aileron installation.

Lift

Section lift, aileron neutral.- Curves of airfoil section lift coefficient c_l plotted against angle of attack α_o are presented in figures 17 to 20. The results indicate that the principal effect on the section lift curve of variations of airspeed, gap width, or balance-nose radii was a change in slope.

Increased airspeed increased the slope of the lift curve as is shown in figures 17, 18, and 21. For a gap width of 0.0055c with the gap both open and sealed, an increase in slope of approximately 15 percent was obtained for the range of test Mach numbers. A slope of 0.124 at a Mach number of 0.473 was obtained from this investigation for the sealed condition. A comparison of the theoretical and the measured effect of Mach number on the slope of the lift curve for the sealed and open gap is given in figure 21. References 6 and 7 show that the slope of the lift curve should vary with Mach number as $\frac{1}{\sqrt{1 - M^2}}$. The theoretical curve in figure 21 was obtained by selecting a value of $\left(\frac{\partial c_l}{\partial \alpha_o}\right)_{\delta_a}$ at zero Mach number of such magnitude that the theoretical increase in lift-curve slope passes through the measured value for the sealed gap at a Mach number of 0.2. The measured effect of Mach number on the slope was greater than the effect indicated by theory. The variation in Reynolds number and the failure to consider compressibility effects in applying the wind-tunnel correction probably contributed to the discrepancy between the theoretical and the measured effect of Mach number.

Increased airspeed had a negligible effect on the angle of zero lift but resulted in separation at a lower angle of attack (figs. 17 and 18).

The effect of gap width on $\left(\frac{\partial c_l}{\partial \alpha_o}\right)_{\delta_a}$ is shown in figure 19. The value $\left(\frac{\partial c_l}{\partial \alpha_o}\right)_{\delta_a}$ was greatest for the sealed gap and only slightly less for the 0.0005c gap width. An increase from 0.0005c to 0.0030c in gap width decreased the value of $\left(\frac{\partial c_l}{\partial \alpha_o}\right)_{\delta_a}$ approximately 8 percent, but a subsequent increase in gap width from 0.0030c to 0.0107c had a negligible effect on the slope. The increased gap width slightly increased the angle of zero lift.

An increase in balance-nose radii from 0 to 0.02c had little effect on the slope of the section lift curve as shown in figure 20.

<u>Section lift, aileron deflected</u>.- Curves of section lift coefficient c_l plotted against aileron angle δ_a are presented in figures 22 to 27. The results, in general, indicate that the lift increased with aileron angle up to some value after which separation occurred, and c_l decreased rapidly.

Although the slopes of the c_l against δ_a curves changed slightly in some cases at $\delta_a = 0$, these slopes generally remained unchanged throughout the unstalled range of aileron deflections. An exception to this condition was found when an effect (probably due to compressibility, Reynolds number, or a combination of both) occurred, which resulted in a rapid decrease in slope with increased aileron deflection. A value of $\left(\frac{\partial c_l}{\partial \delta_a}\right)_{\alpha_o}$ of 0.045 was obtained as an approximate average slope for all test conditions in the unstalled range of aileron deflections.

The principal effects of increased airspeed were an appreciable decrease in the range of aileron angles over which lift effectiveness was maintained and a decrease, generally, in the maximum value of c_l. (See figs. 22 to 27.)

The effect of airspeed on $\left(\frac{\partial c_l}{\partial \delta_a}\right)_{\alpha_o}$ is shown in figures 28 to 31. At $\alpha_o = 0^\circ$ and 5° for all Mach numbers and at $\alpha_o = -5^\circ$ and 10° for low Mach numbers, the value of $\left(\frac{\partial c_l}{\partial \delta_a}\right)_{\alpha_o}$ increased with Mach number, as is shown in figures 28 and 29. As the Mach numbers increased above 0.35, the value of $\left(\frac{\partial c_l}{\partial \delta_a}\right)_{\alpha_o}$ remained about constant for $\alpha_o = -5^\circ$ and rapidly decreased for $\alpha_o = 10^\circ$. This change was probably a compressibility effect. The value of $\left(\frac{\partial c_l}{\partial \delta_a}\right)_{\alpha_o}$ varied with α_o, but the rate of increase with Mach number below critical speeds was approximately the same for all values of α_o. The results of this investigation indicate that at zero angle of attack the effect of airspeed on both the aileron effectiveness and the balance effectiveness was slight.

Variations in gap width generally had a negligible effect on the range of aileron angles over which lift effectiveness was maintained (figs. 23 to 27). Increased gap width, however, did appreciably decrease the maximum value of c_l. The effect of gap width on $\left(\frac{\partial c_l}{\partial \delta_a}\right)_{\alpha_o}$ is shown in figure 30. At zero angle of attack the value of $\left(\frac{\partial c_l}{\partial \delta_a}\right)_{\alpha_o}$ decreased with increased gap width; however, at $\alpha_o = 10^\circ$ the effect of gap width on $\left(\frac{\partial c_l}{\partial \delta_a}\right)_{\alpha_o}$ depended on the airspeed. For low airspeeds the effect is similar to that for zero angle of attack, but at high airspeeds the value of $\left(\frac{\partial c_l}{\partial \delta_a}\right)_{\alpha_0}$ increased with gap width. (See fig. 30.) At high airspeeds and zero angle of attack for the condition at which the best hinge-moment balance was obtained, that is, for a gap width of approximately 0.01c and $\left(\frac{\partial c_{h_a}}{\partial \delta_a}\right)_{\alpha_0} = -0.0002$, the value of $\left(\frac{\partial c_l}{\partial \delta_a}\right)_{\alpha_0} = 0.042$ was the smallest for the range of gap widths tested.

Increased balance-nose radii greatly increased the range of aileron deflections over which lift effectiveness was maintained and appreciably increased the maximum value of c_l. (See figs. 22 and 25.) The effect of balance-nose radii on $\left(\frac{\partial c_l}{\partial \delta_a}\right)_{\alpha_0}$ is somewhat irregular as can be seen from figure 31.

Pitching-Moment Coefficient

The variation of the airfoil section pitching-moment coefficient $c_{m_{c/4}}$ with angle of attack α_0, aileron neutral, which was obtained from pressure distribution, is presented in figure 32. The principal effect on the $c_{m_{c/4}}$ curve of a variation of airspeed or gap width was a change in slope, whereas the effect of balance-nose radii was negligible; increased gap width or increased airspeed increased the slope of the $c_{m_{c/4}}$ curve. The variation was approximately linear and was sufficient to double the slope for the range of test Mach numbers and gap widths.

CONCLUSIONS

From the results of this investigation the following conclusions may be drawn:

1. Increased airspeed increased the positive slope of the airfoil section lift curves and pitching-moment-coefficient

curves, increased the slope of the curves of section lift coefficient with aileron angle, and had a negligible effect on the balance effectiveness at low angles of attack for small aileron angles. The unstalled range of aileron deflections decreased with increased speed.

2. Increased gap width increased the aileron balance effectiveness but decreased the slope of the curves of section lift coefficient with aileron angles at low angles of attack for small aileron angles. An increase in gap width usually decreased the slope of the airfoil section lift curve but increased the positive slope of the airfoil section pitching-moment-coefficient curve.

3. Increased balance-nose radii greatly increased the unstalled range of aileron angles and decreased the balance effectiveness for small angles.

Langley Memorial Aeronautical Laboratory,
National Advisory Committee for Aeronautics,
Langley Field, Va.

REFERENCES

1. Letko, W., Denaci, H. G., and Freed, C.: Wind-Tunnel Tests of Ailerons at Various Speeds. I - Ailerons of 0.20 Airfoil Chord and True Contour with 0.35 Aileron-Chord Extreme Blunt Nose Balance on the NACA 66,2-216 Airfoil. NACA ACR No. 3F11, 1943.

2. Donaci, H. G., and Bird, J. D.: Wind-Tunnel Tests of Ailerons at Various Speeds. II - Ailerons of 0.20 Airfoil Chord and True Contour with 0.60 Aileron-Chord Sealed Internal Balance on the NACA 66,2-216 Airfoil. NACA ACR No. 3F18, 1943.

3. Letko, W. and Kemp, W.: Wind-Tunnel Tests of Ailerons at Various Speeds. III - Ailerons of 0.20 Airfoil Chord and True Contour with 0.35 Aileron-Chord Frise Balance on the NACA 23012 Airfoil. NACA ACR No. 3I14, 1943.

4. Pursor, Paul E., and Toll, Thomas A.: Wind-Tunnel Investigation of the Characteristics of Blunt-Nose Ailerons on a Tapered Wing. NACA ARR, Feb. 1943.

5. Wenzinger, Carl J., and Delano, James B.: Pressure Distribution over an N.A.C.A. 23012 Airfoil with a Slotted and a Plain Flap. NACA Rep. No. 633, 1938.

6. Glauert, H.: The Effect of Compressibility on the Lift of an Aerofoil. R. & M. No. 1135, British A.R.C. 1928.

7. Ackert, L. J.: Über Luftkräfte bei sehr grossen Geschwindigkeiten insbesondere bei ebenen Strömungen. Helvetica Physica Acta, vol. I, fasc. 5, 1928, pp. 301-322.

8. Purser, Paul E., and McKee, John W.: Wind-Tunnel Investigation of a Plain Aileron with Thickened and Beveled Trailing Edges on a Tapered Low-Drag Wing. NACA ACR, Jan. 1943.

TABLE I

LIST OF FIGURES

Figure	Variation shown	Mach number (approx.)	Balance-nose radii	Gap width
5	c_{h_a} against δ_a; $\alpha_o = -5.1^\circ$, 0°, 5.1°, 10.2°	0.197, .289, .357, .416, .453	0.01c	0.0055c
6			.02c	.0005c
7			.02c	.0030c
8			.02c	.0055c
9			.02c	.0055c(sealed)
10			.02c	.0107c
11	$\left(\frac{\partial c_{h_a}}{\partial \delta_a}\right)_{\alpha_o}$ against M; $\alpha_o = -5.1^\circ$, 0°, 5.1°, 10.2°	Varies	.02c	.0055c
12		Varies	.02c	.0055c(sealed)
13	$\left(\frac{\partial c_{h_a}}{\partial \delta_a}\right)_{\alpha_o}$ against gap width; $\alpha_o = 0^\circ$, 10°	.197, .417	.02c	0 to .0120c
14	$\left(\frac{\partial c_{h_a}}{\partial \delta_a}\right)_{\alpha_o}$ against nose radii; $\alpha_o = 0^\circ$, 10°	.197, .417	0 to .02c	.0055c(sealed)
15	c_{h_a} against α_o; $\delta_a = 0^\circ$, $\pm 13^\circ$	.197, .417	.02c	.0055c
16			.02c	(sealed)
17	c_l against α_o; $\delta_a = 0^\circ$	.197, .289	.02c	.0055c
18		.357, .416, .453	.02c	.0055c(sealed)
19	c_l against α_o	.417	.02c	.0005c .0030c .0055c .0055c(sealed) .0107c

TABLE I - LIST OF FIGURES (Continued)

Figure	Variation shown	Mach number (approx.)	Balance-nose radii	Gap width
20	c_l against α_o	0.417	0.00c .01c .02c	0.0055c(sealed)
21	$\left(\frac{\partial c_l}{\partial \alpha_o}\right)_{\delta_a}$ against M	Varies	.02c	.0055c .0055c(sealed)
22	c_l against δ_a; α_o = -5.1°, 0°, 5.1°, 10.2°	.197, .289, .357, .416, .453	.01c	.0055c
23			.02c	.0005c
24			.02c	.0030c
25			.02c	.0055c
26			.02c	.0055c(sealed)
27			.02c	.0107c
28	$\left(\frac{\partial c_l}{\partial \delta_a}\right)_{\alpha_o}$ against M; α_o = -5.1°, 0°, 5.1°, 10.2°	Varies	.02c	.0055c
29			.02c	.0055c(sealed)
30	$\left(\frac{\partial c_l}{\partial \delta_a}\right)_{\alpha_o}$ against gap width; α_o = 0°, 10°	.199, .417	.02c	0 to .0120c
31	$\left(\frac{\partial c_l}{\partial \delta_a}\right)_{\alpha_o}$ against nose radii; α_o = 0°, 10°	.199, .417	0 to .02c	.0055c .0055c(sealed)
32	$c_{m_{c/4}}$ against α_o; δ_a = 0°	.199, .358, .473	.01c .02c	.0005c .0030c .0055c .0055c(sealed)

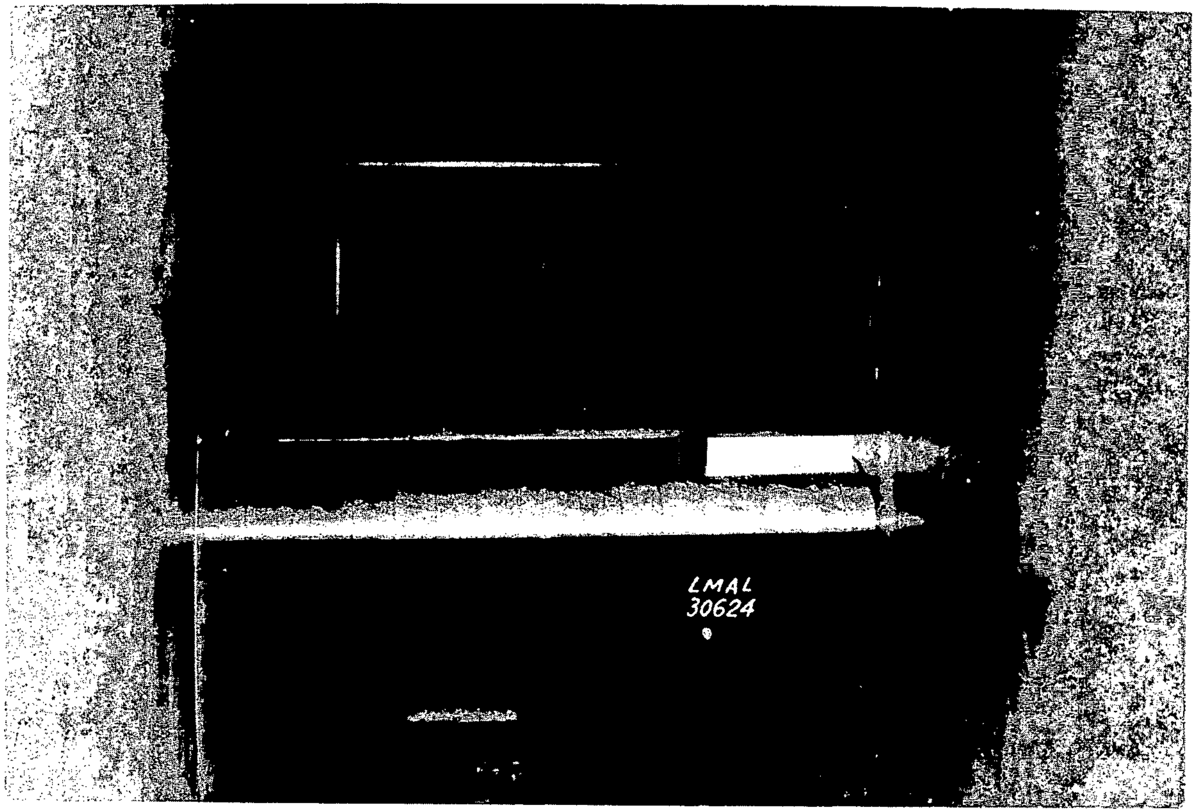

Figure 1.- Airfoil and aileron mounted in tunnel.

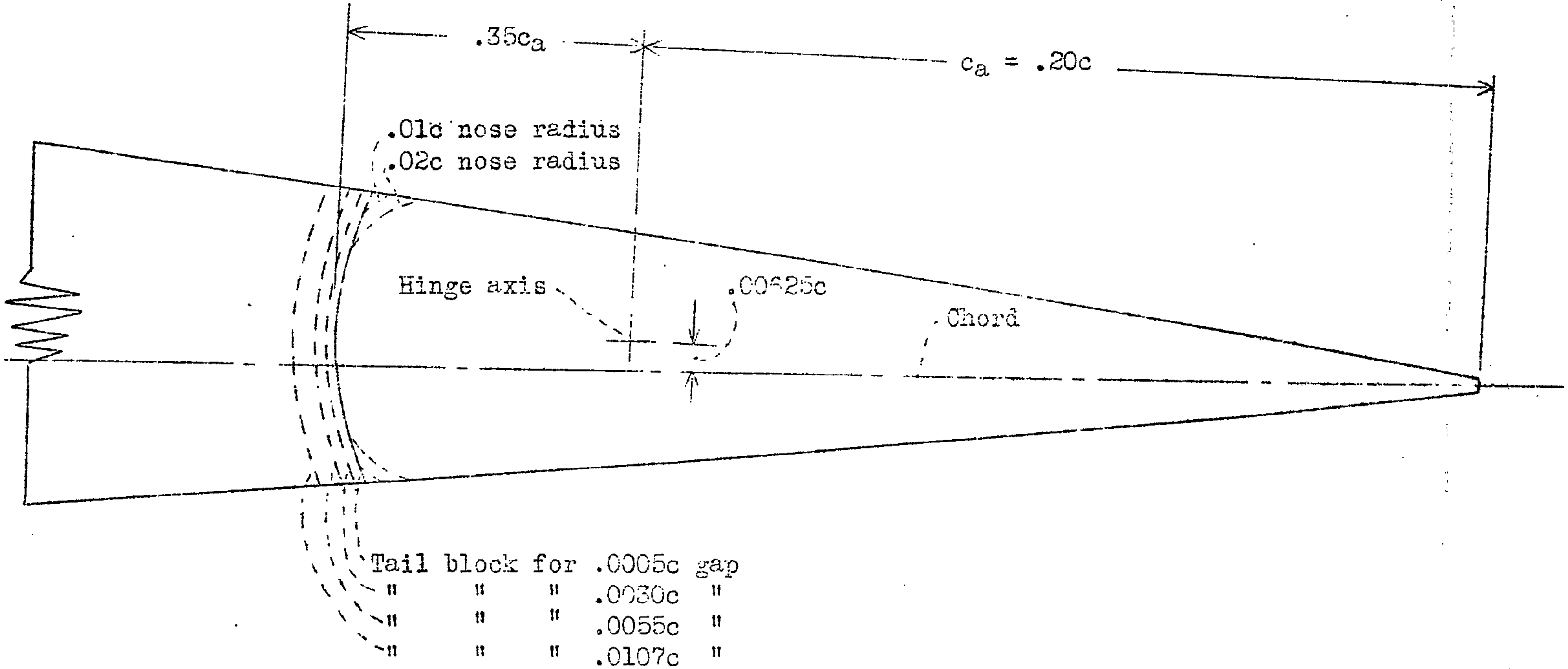

Figure 2.- Aileron section of an NACA 23012 airfoil showing test variations of aileron-nose shapes and gaps.

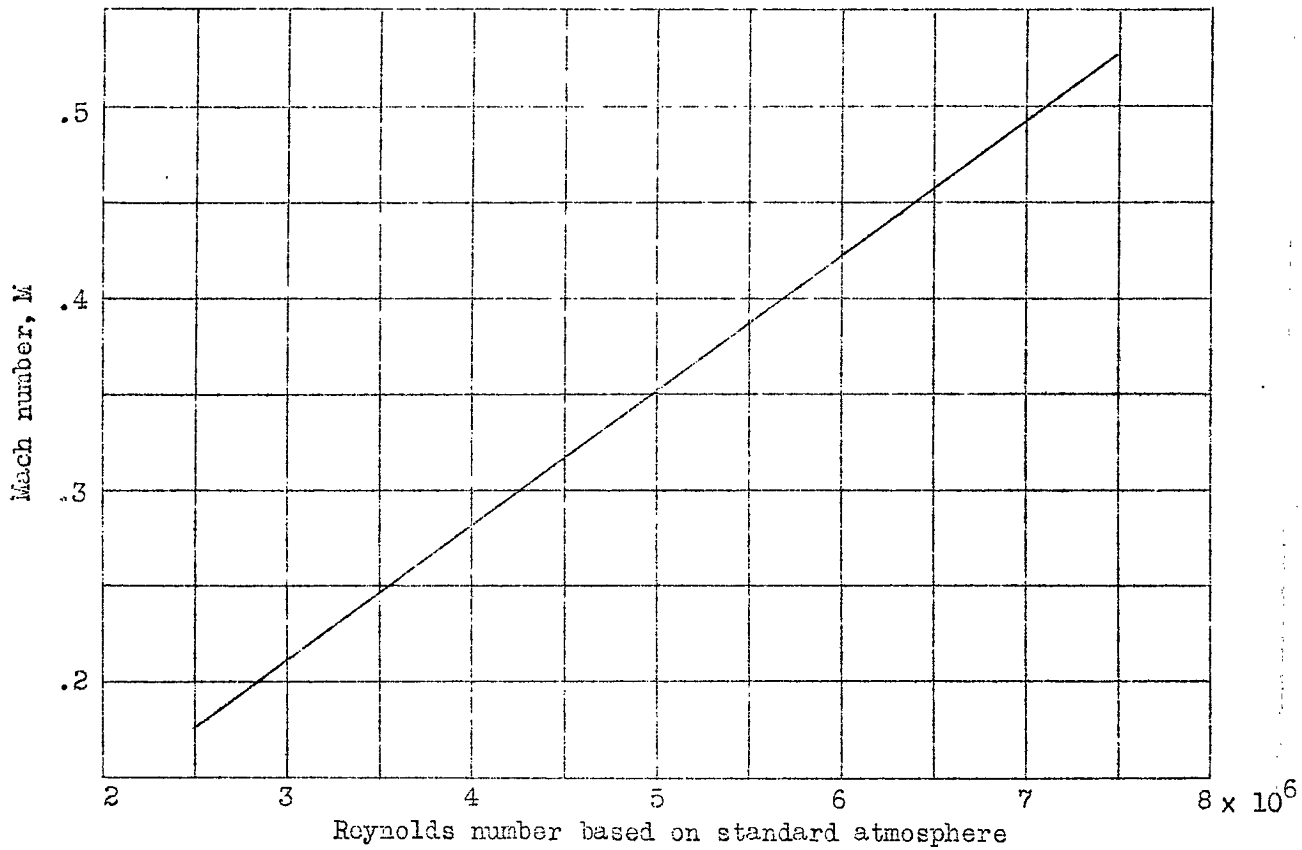

Figure 3.- Reynolds number for values of test Mach number for a 2-foot chord airfoil in the 2.5-by 6-foot test section of the stability tunnel.

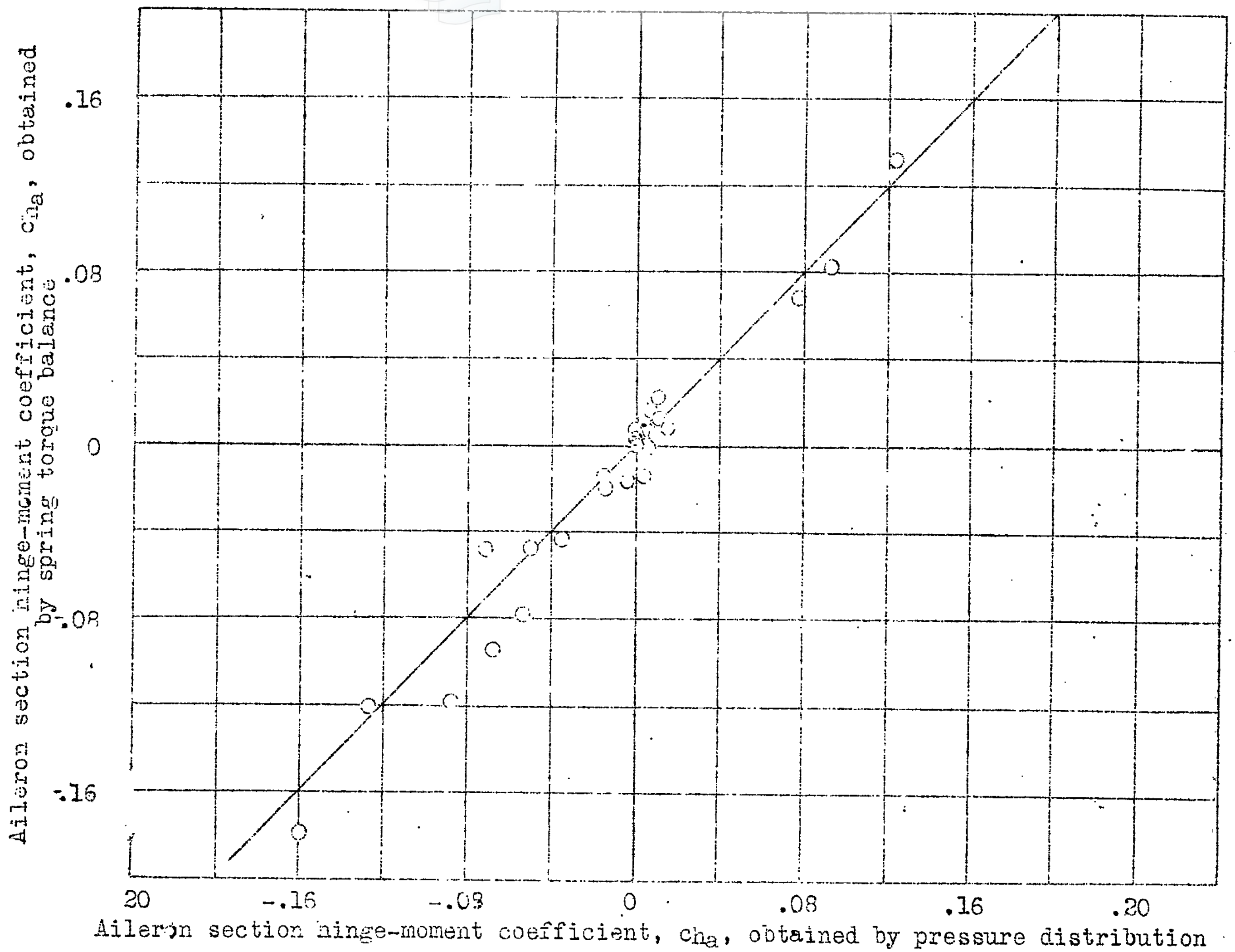

Figure 4.- A comparison between spring-balance and pressure-distribution section hinge-moment coefficients.

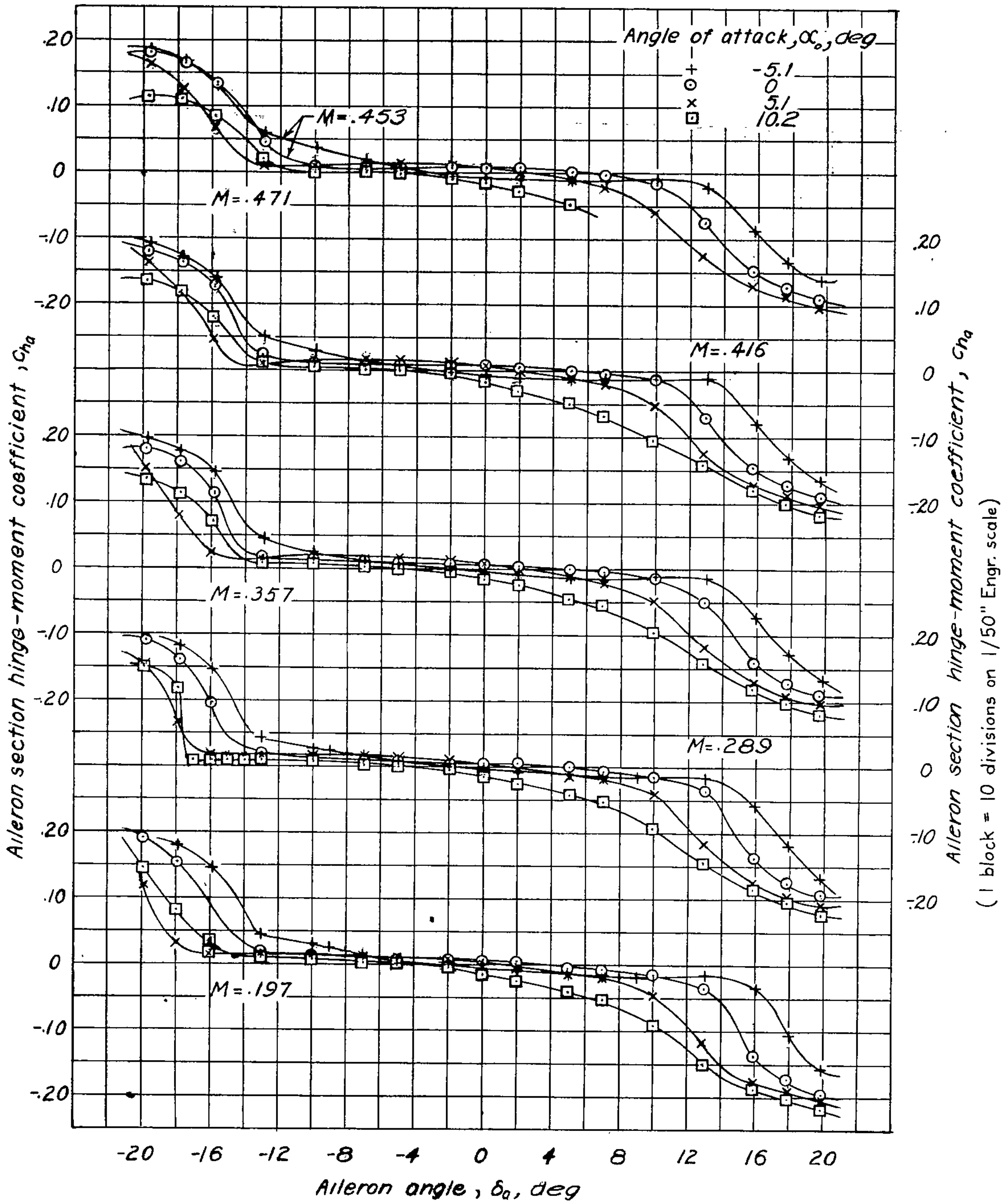

Figure 5.—Variation of aileron section hinge-moment coefficient with aileron angle. Nose radii = 0.01c; gap width = 0.0055c.

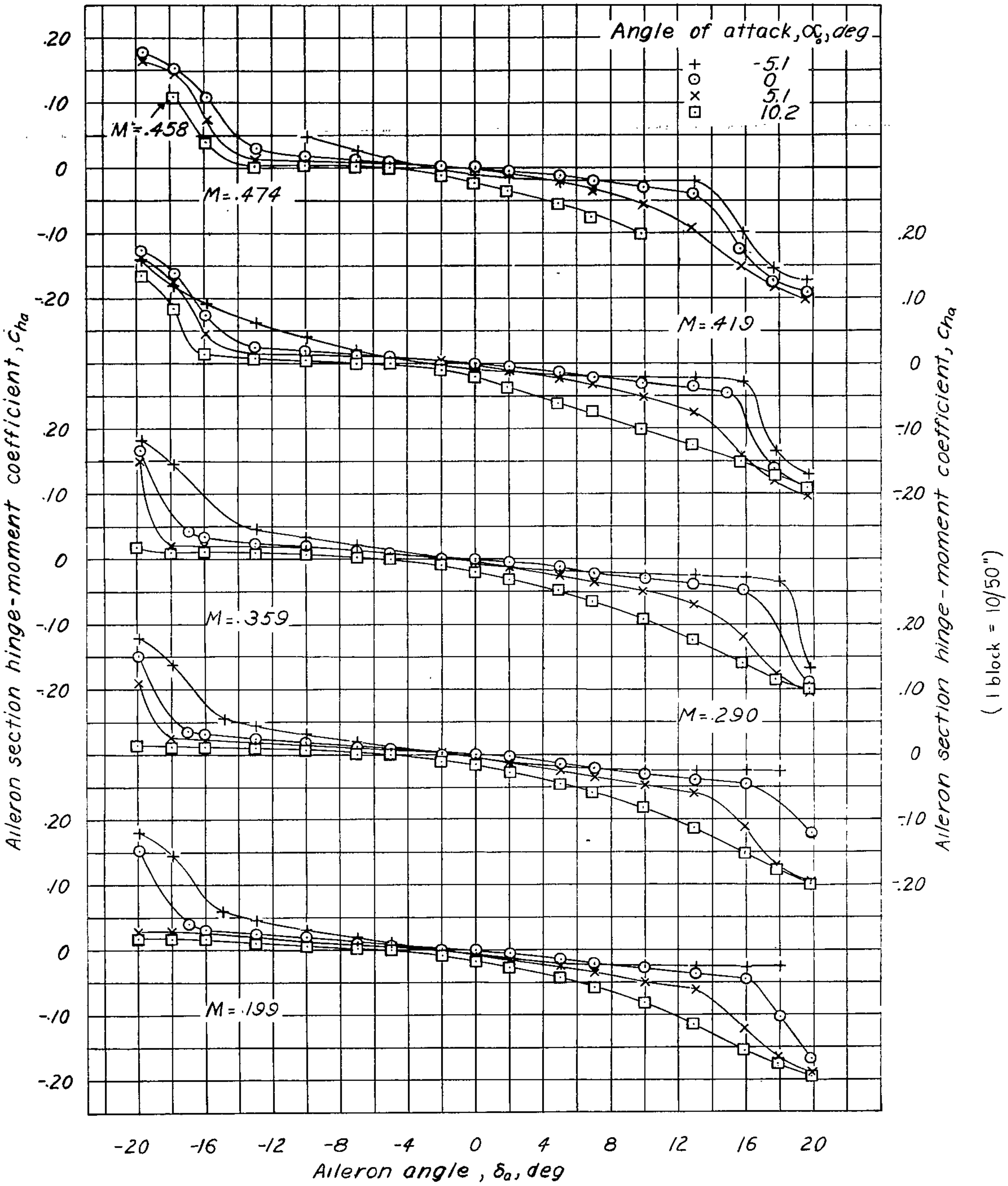

Figure 6.—Variation of aileron section hinge-moment coefficient with aileron angle. Nose radii = 0.02 c; gap width = 0.0005c.

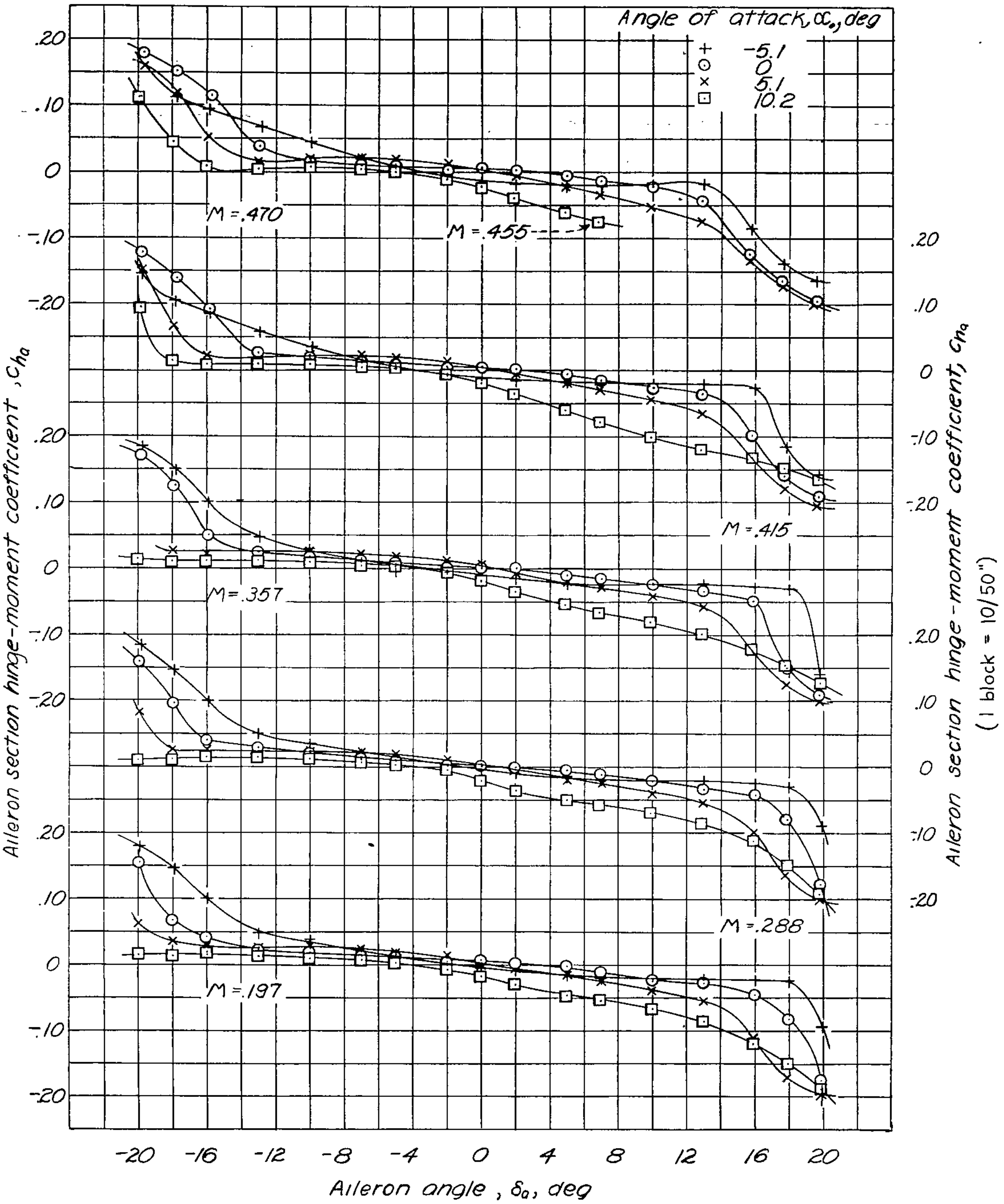

Figure 7.—Variation of aileron section hinge-moment coefficient with aileron angle. Nose radii = 0.02c; gap width = 0.0030c.

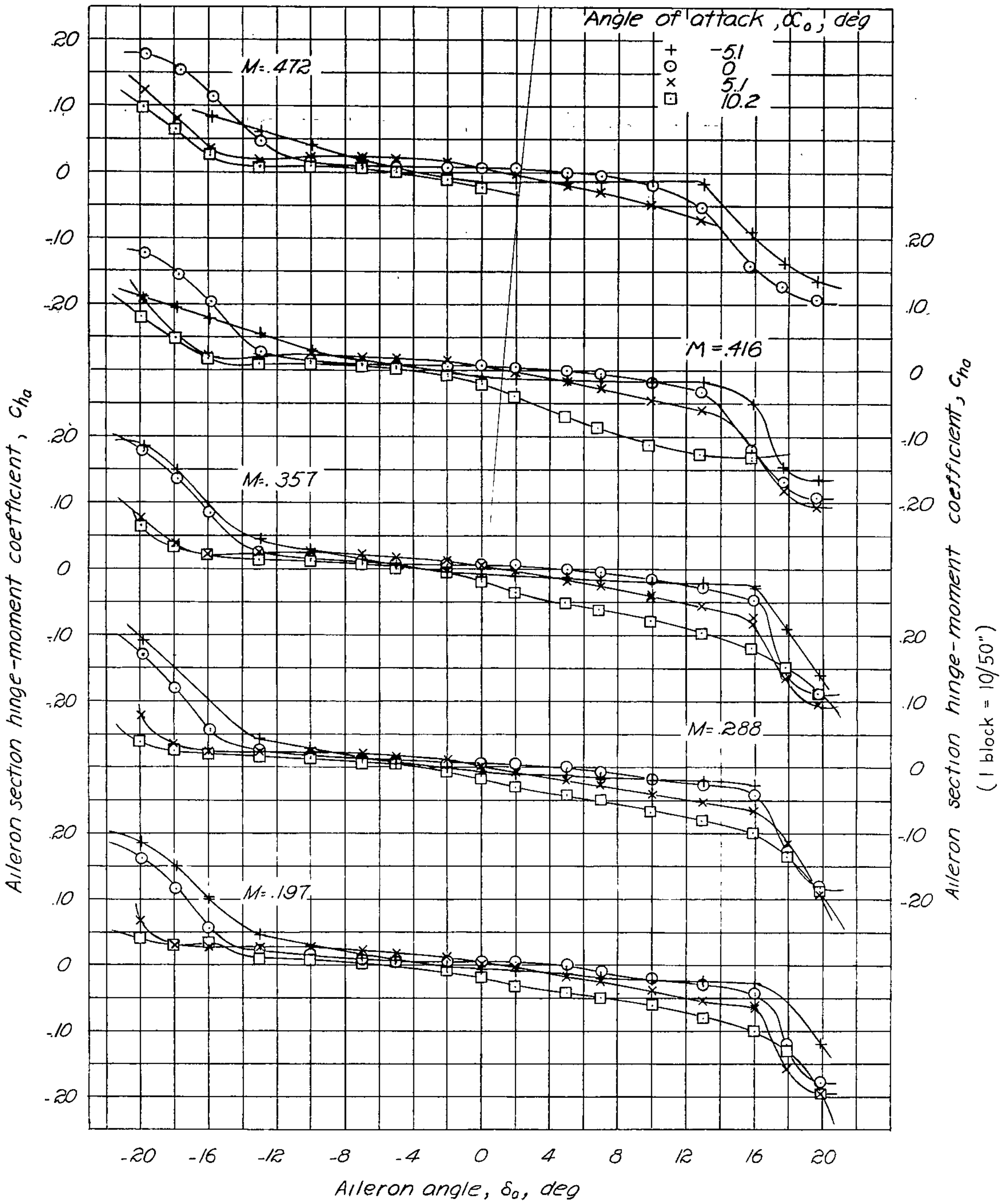

Figure 8.—Variation of aileron section hinge-moment coefficient with aileron angle. Nose radii = 0.02c; gap width = 0.0055c.

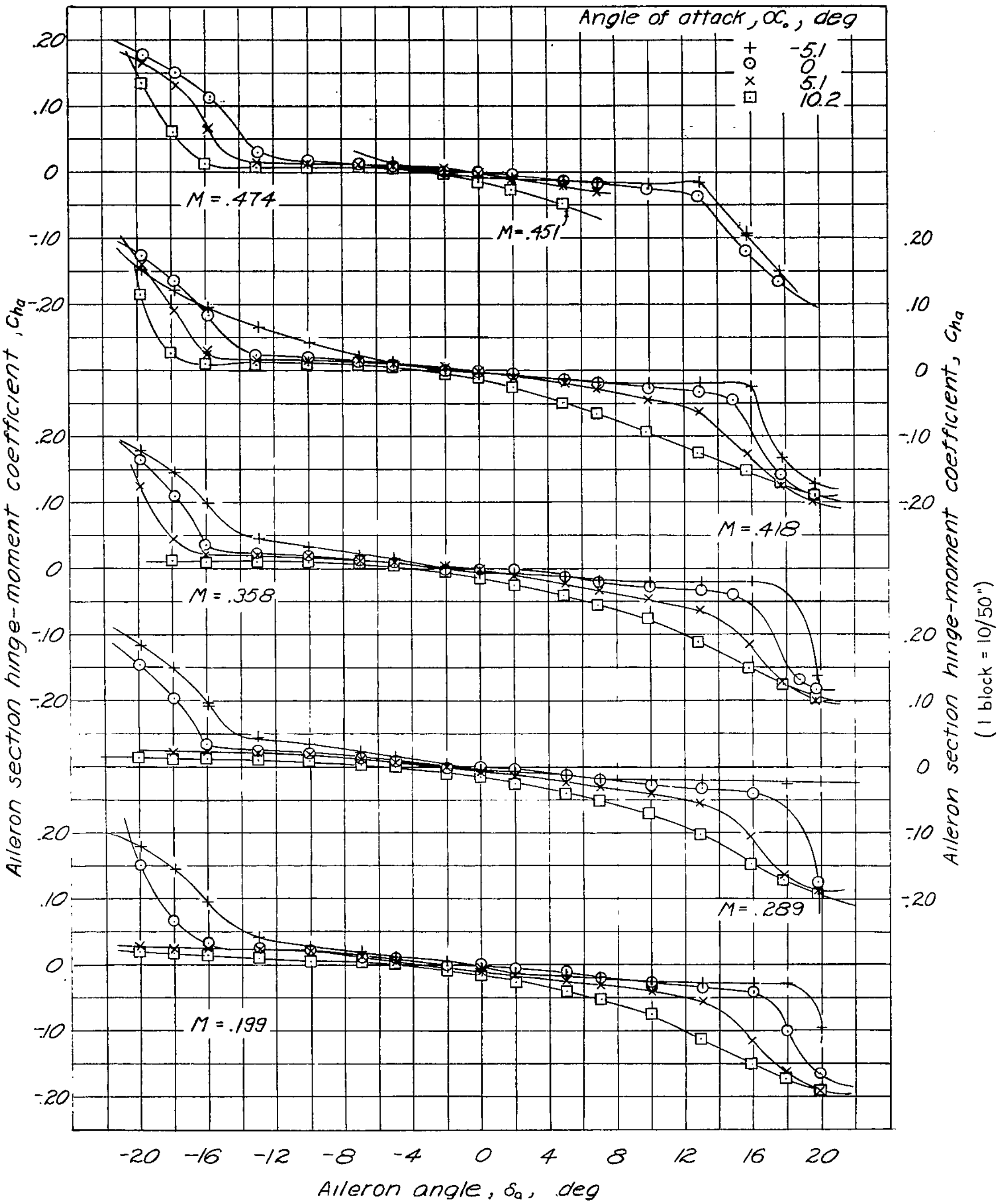

Figure 9.—Variation of aileron section hinge-moment coefficient with aileron angle. Nose radii = 0.02c; gap width = 0.0055c (sealed).

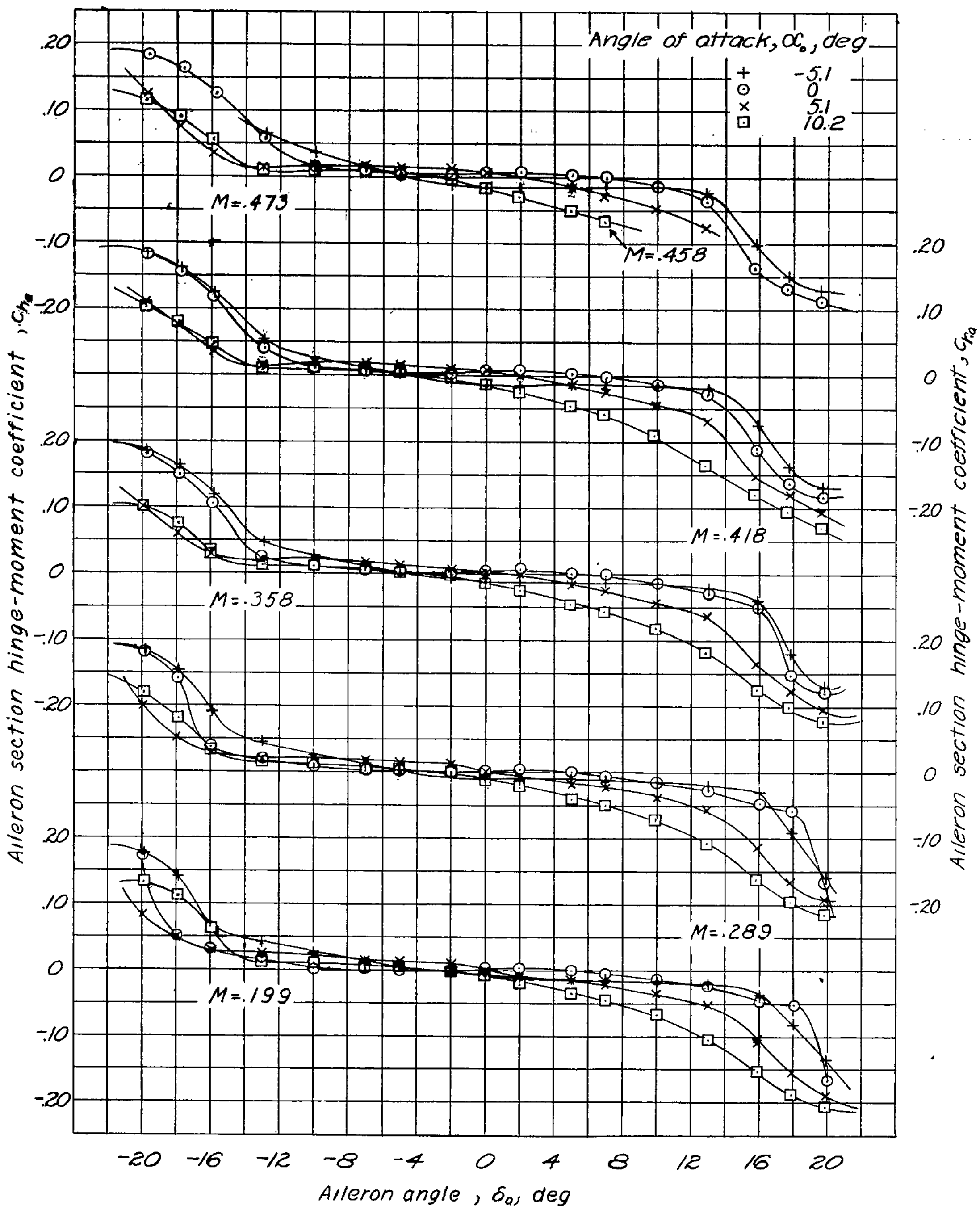

Figure 10.— Variation of aileron section hinge-moment coefficient with aileron angle. Nose radii = 0.02c; gap width = 0.0107c.

L-433

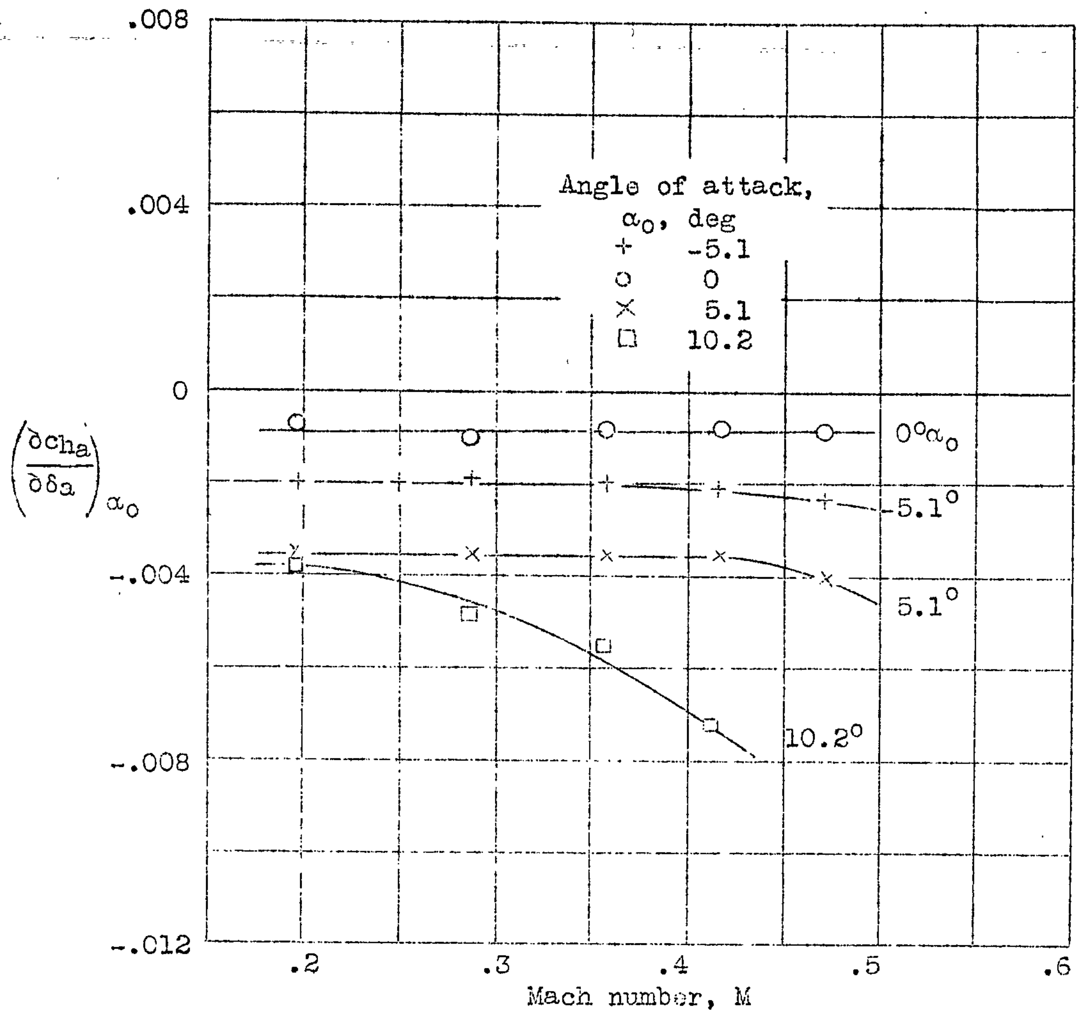

Figure 11.- Effect of Mach number on the slope of the curve of hinge-moment coefficient with aileron angle. Gap width = 0.0055c; nose radii = 0.02c.

L-433

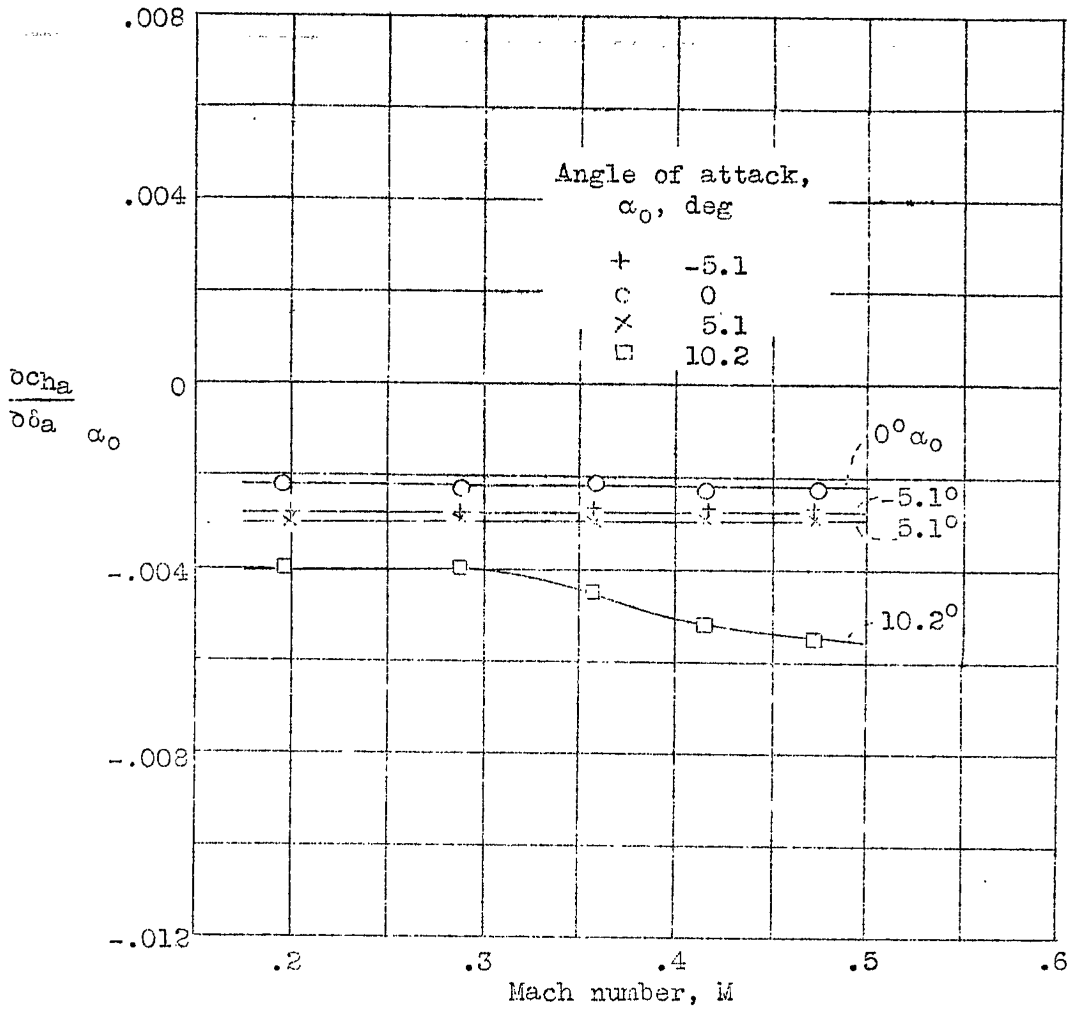

Figure 12.- Effect of Mach number on the slope of the curve of hinge-moment coefficient with aileron angle. Gap width = 0.0055c (sealed); nose radii = 0.02c.

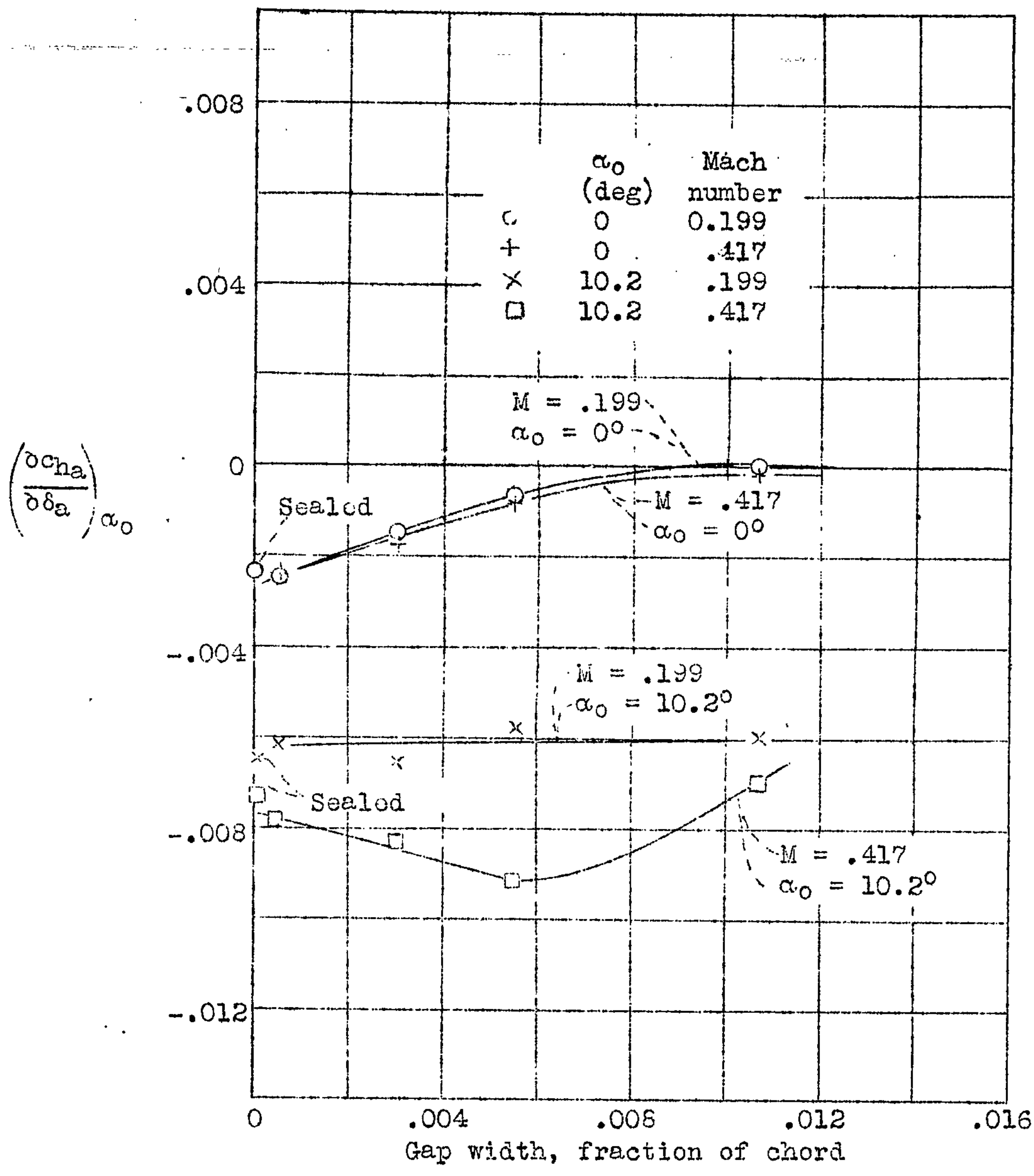

Figure 13.- Effect of gap width on the slope of the curve of hinge-moment coefficient with aileron angle. Nose radii = 0.02c.

L-433

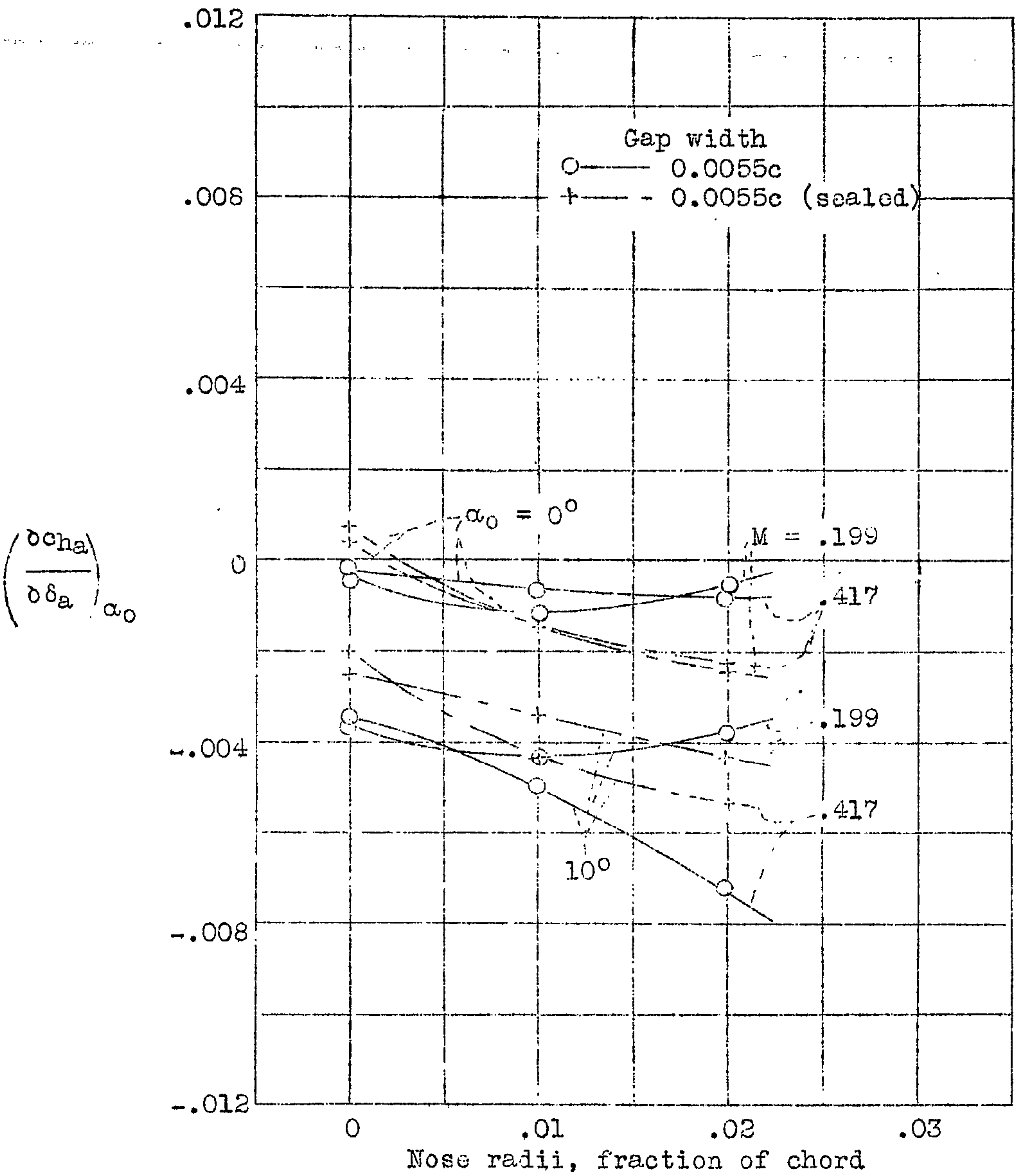

Figure 14.- Effect of nose radii on the slope of the curve of hinge-moment coefficient with aileron angle.

L-433

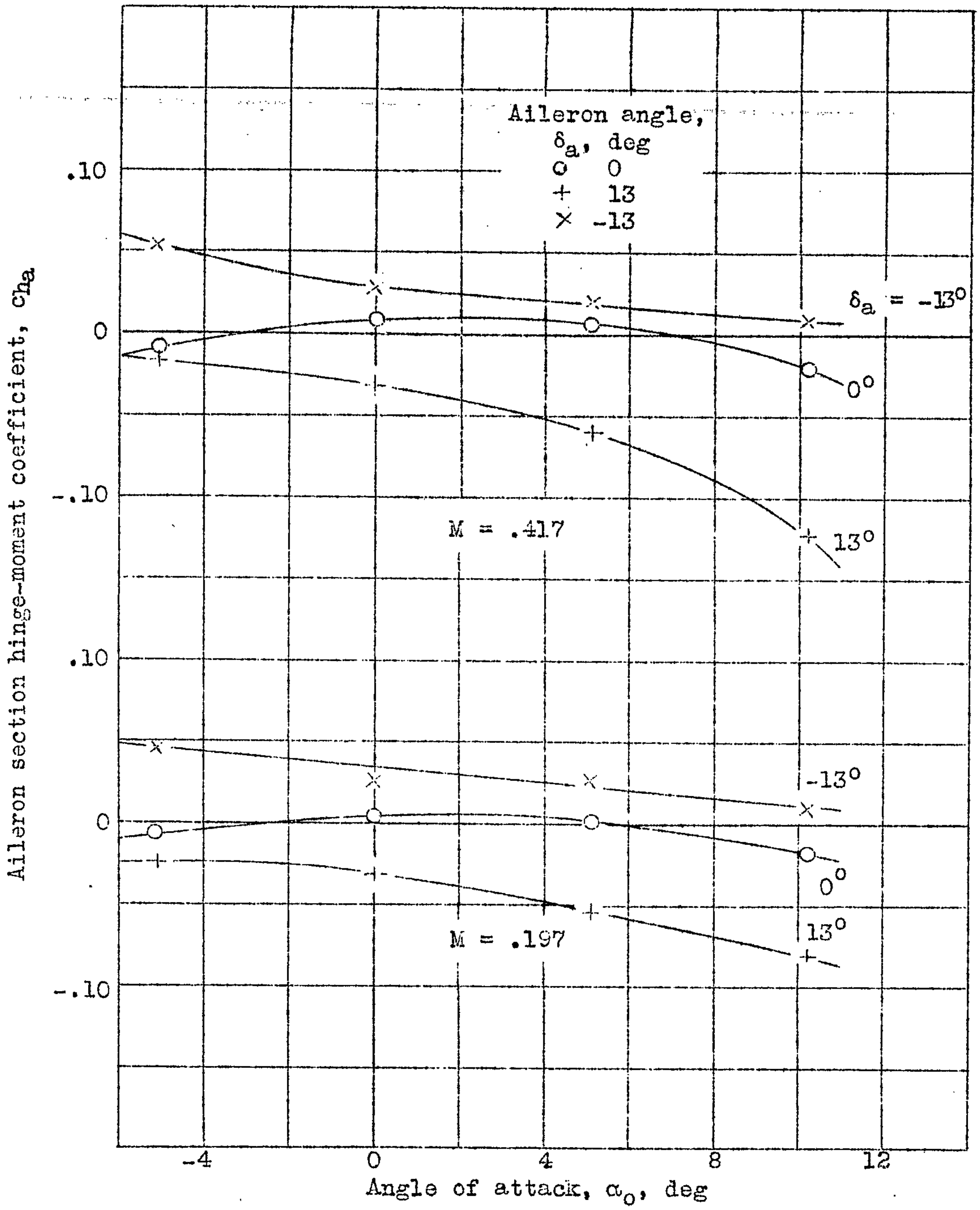

Figure 15.- Variation of aileron section hinge-moment coefficient with angle of attack. Gap width = 0.0055c; nose radii = 0.02c.

L-433

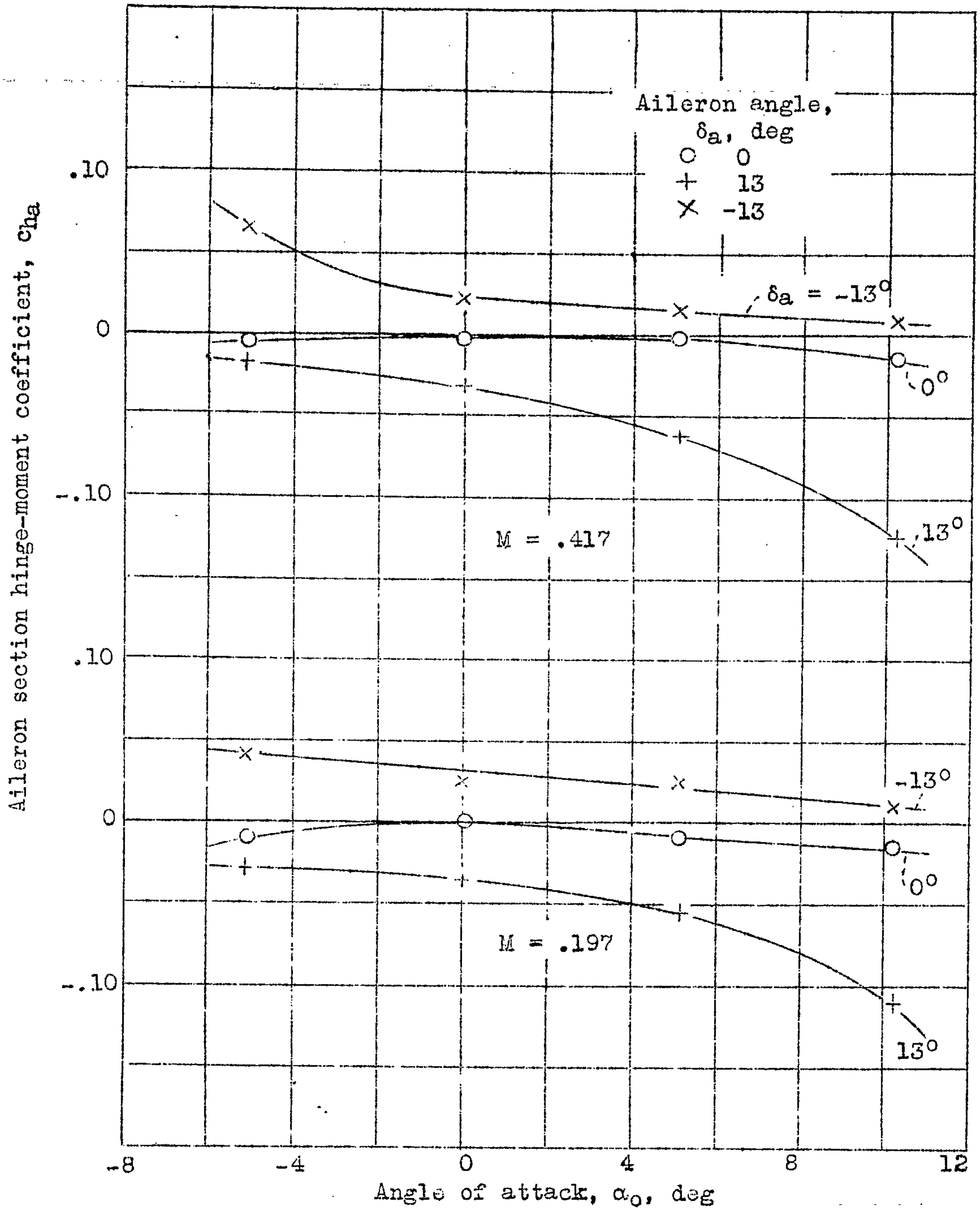

Figure 16.- Variation of aileron section hinge-moment coefficient with angle of attack. Gap width = 0.0055c (sealed); nose radii = 0.02c.

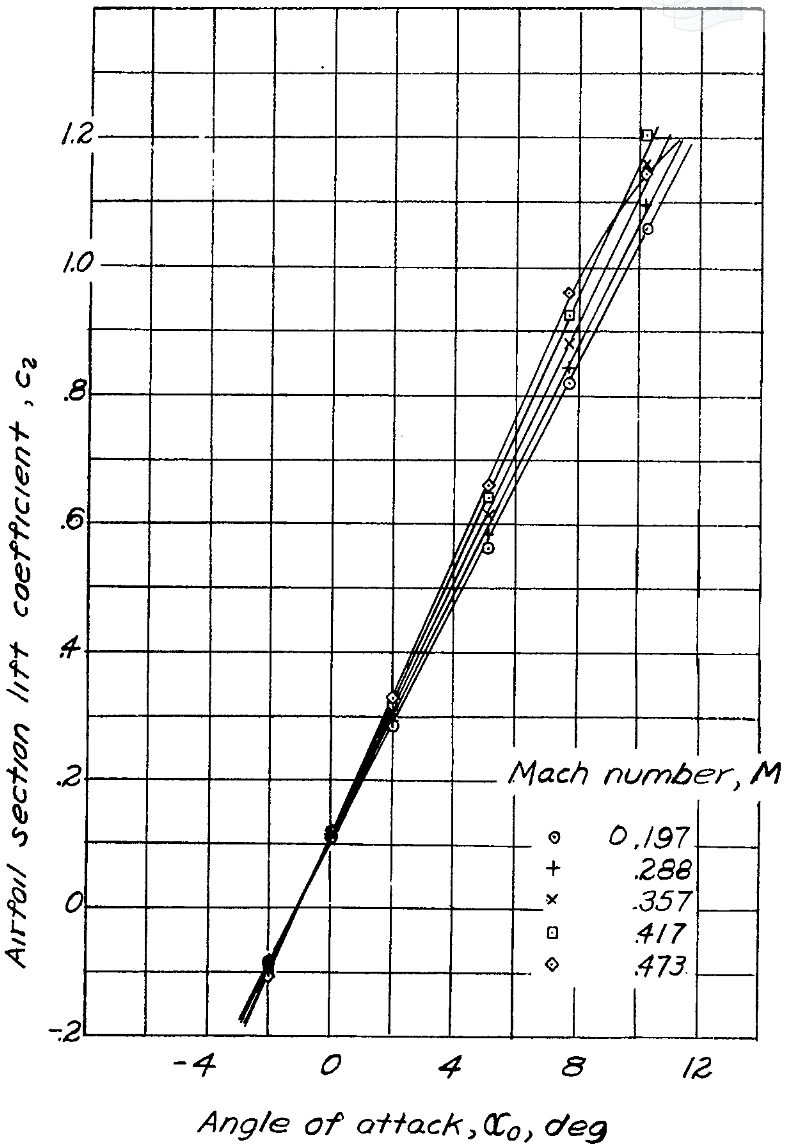

Figure 17.- Effect of variation of Mach number on slope of lift curve, $\delta_a = 0^\circ$. Nose radii = 0.02c; gap width = 0.0055c.

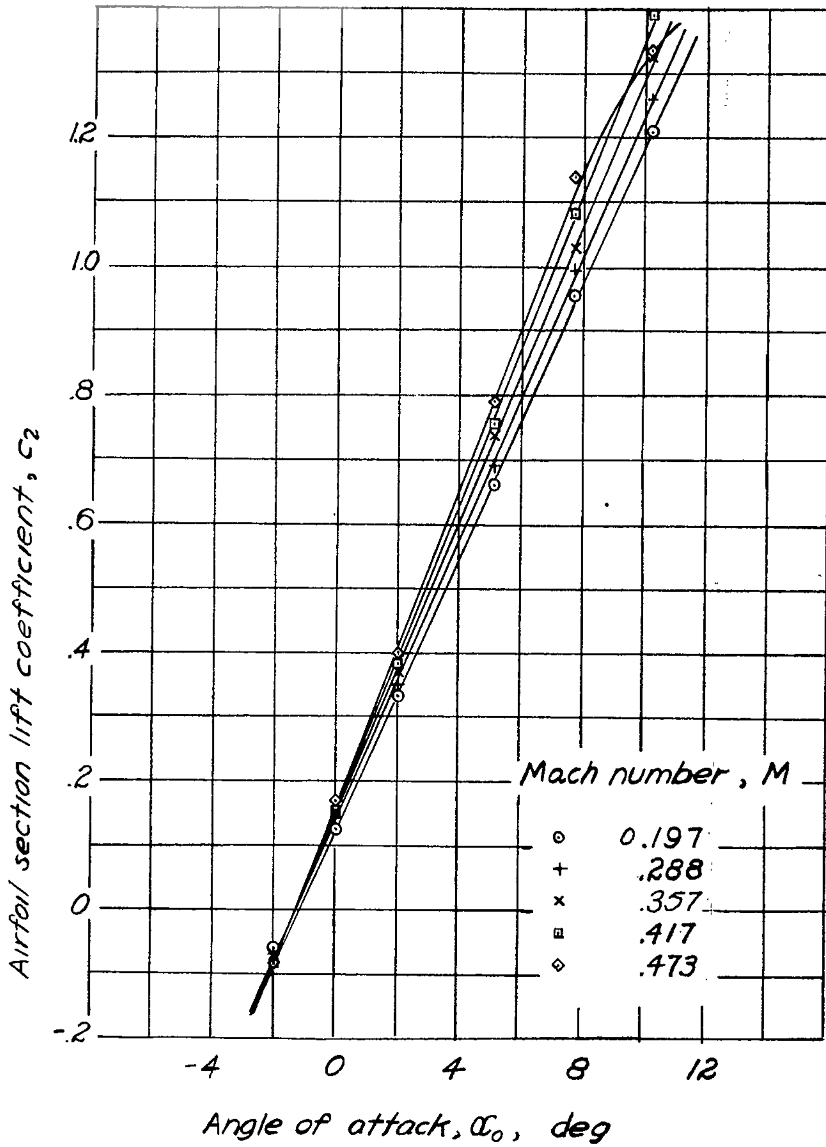

Figure 18.- Effect of variation of Mach number on slope of lift curve, $\delta_a = 0^\circ$. Nose radii = 0.02c; gap width = 0.0055c (sealed).

(1 block = 10 divisions on 1/30" Engr. scale)

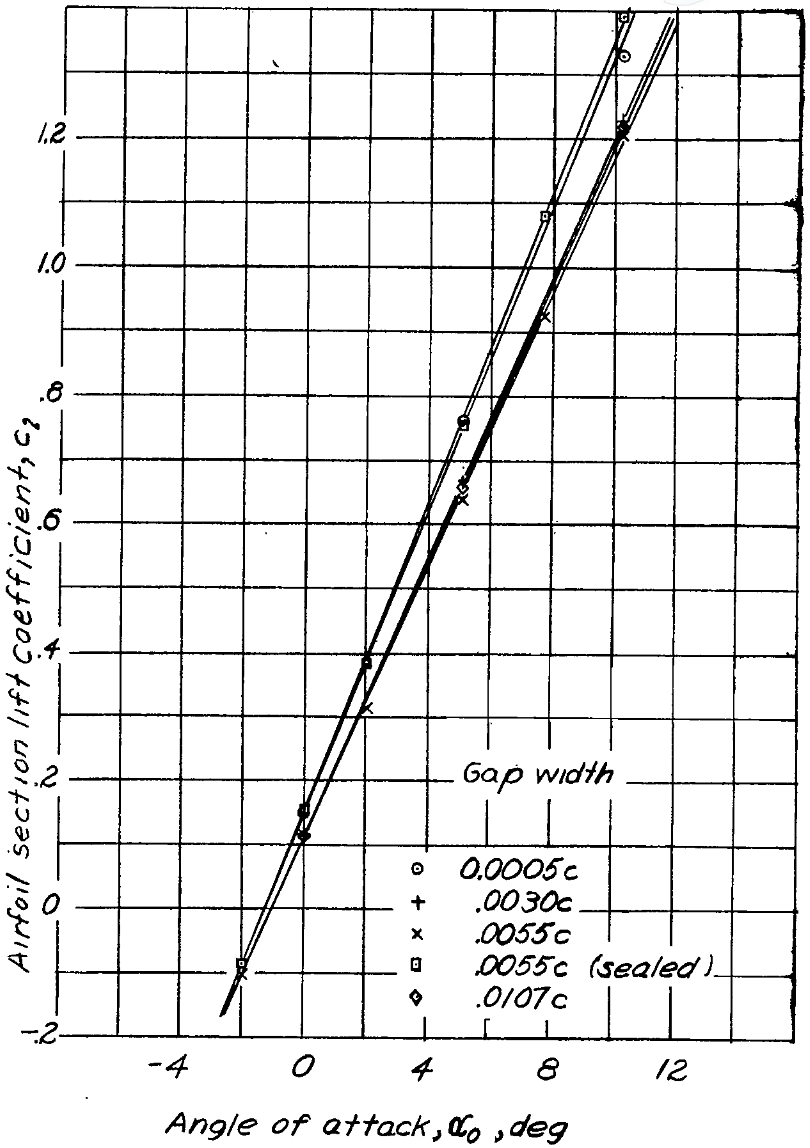

Figure 19.- Effect of variation of gap width on slope of lift curve, $\delta_a = 0°$. Nose radii = 0.02c; Mach number = 0.417

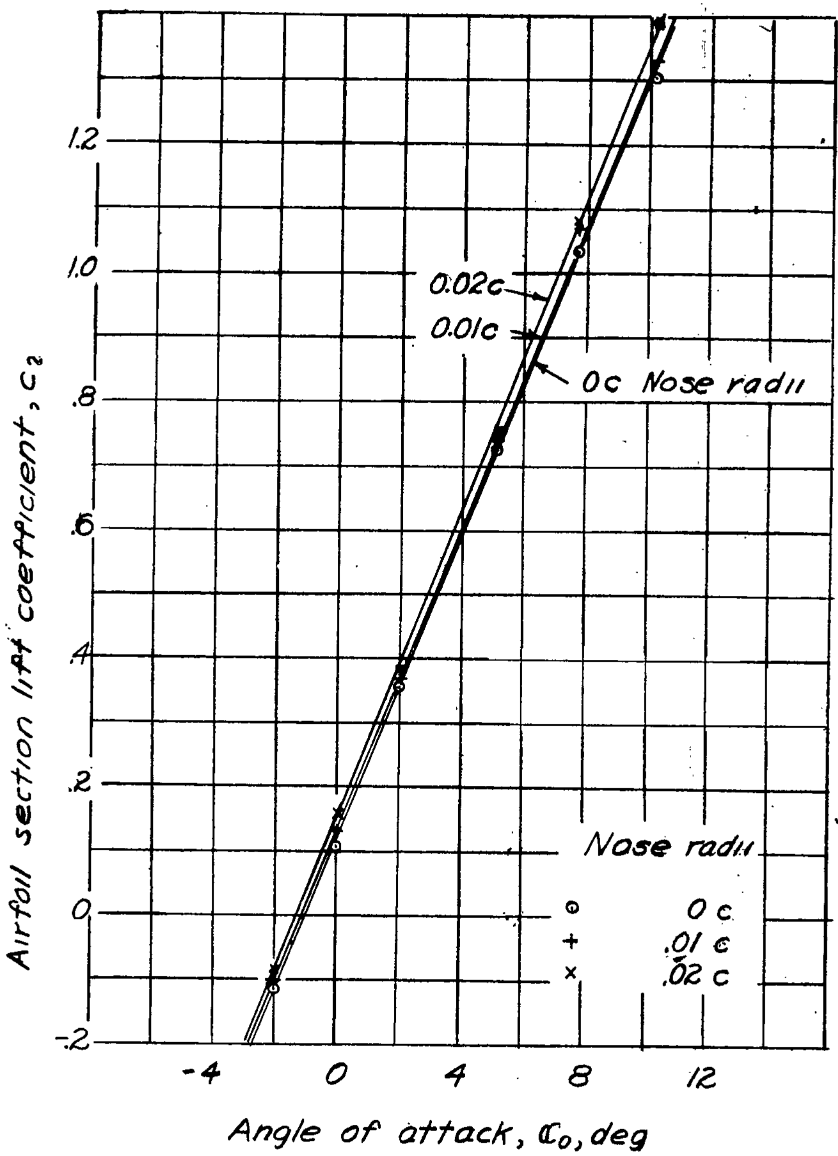

Figure 20.- Effect of variation of aileron nose radii on slope of lift curve; $\delta_a = 0°$. Gap width = 0.0055c sealed; Mach number = 0.417

(1 block = 10 divisions on 1/30" Engr. scale)

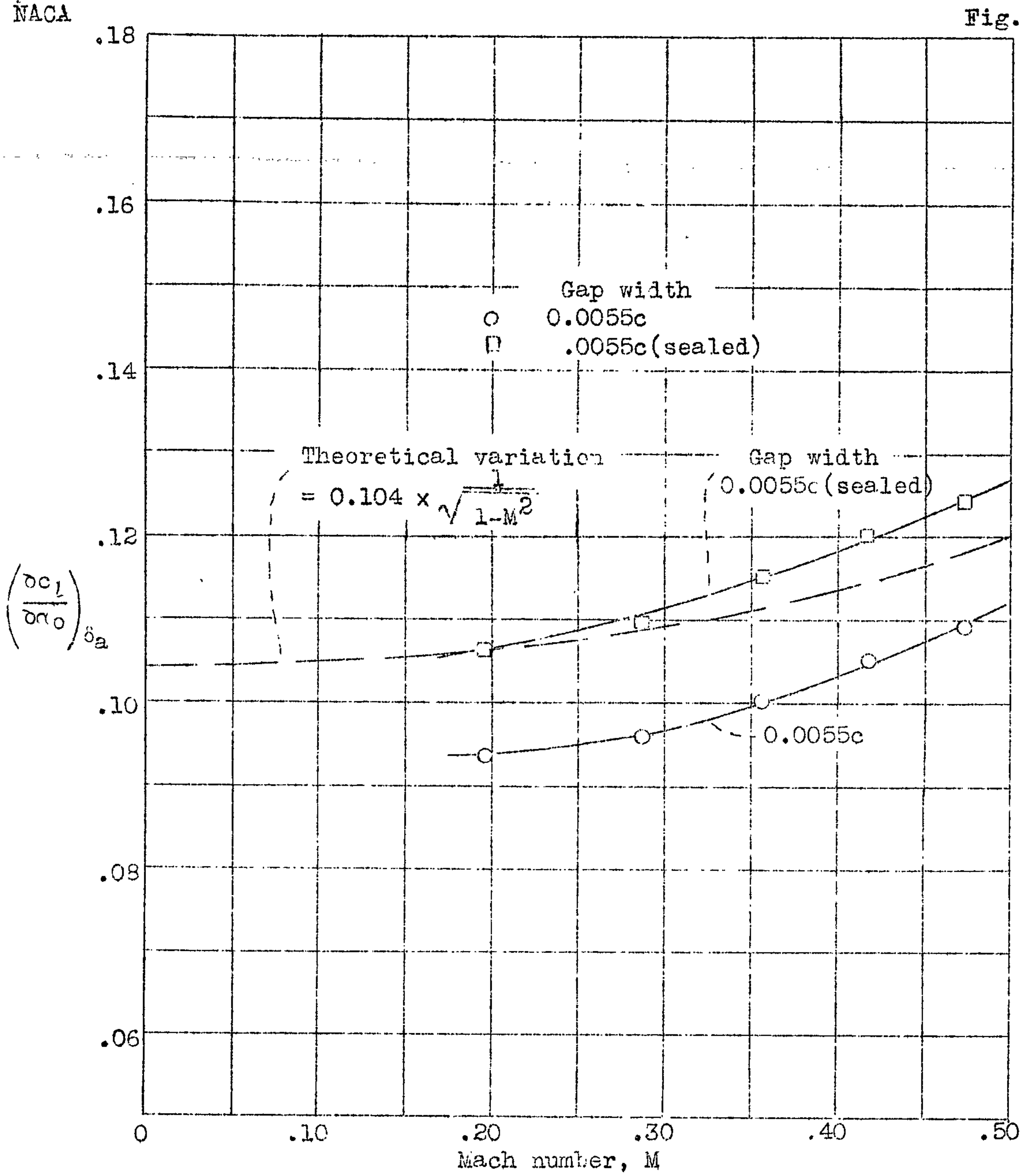

Figure 21.- Comparison of theoretical and measured effect of Mach number on the slope of the lift curve. Nose radii = 0.02c.

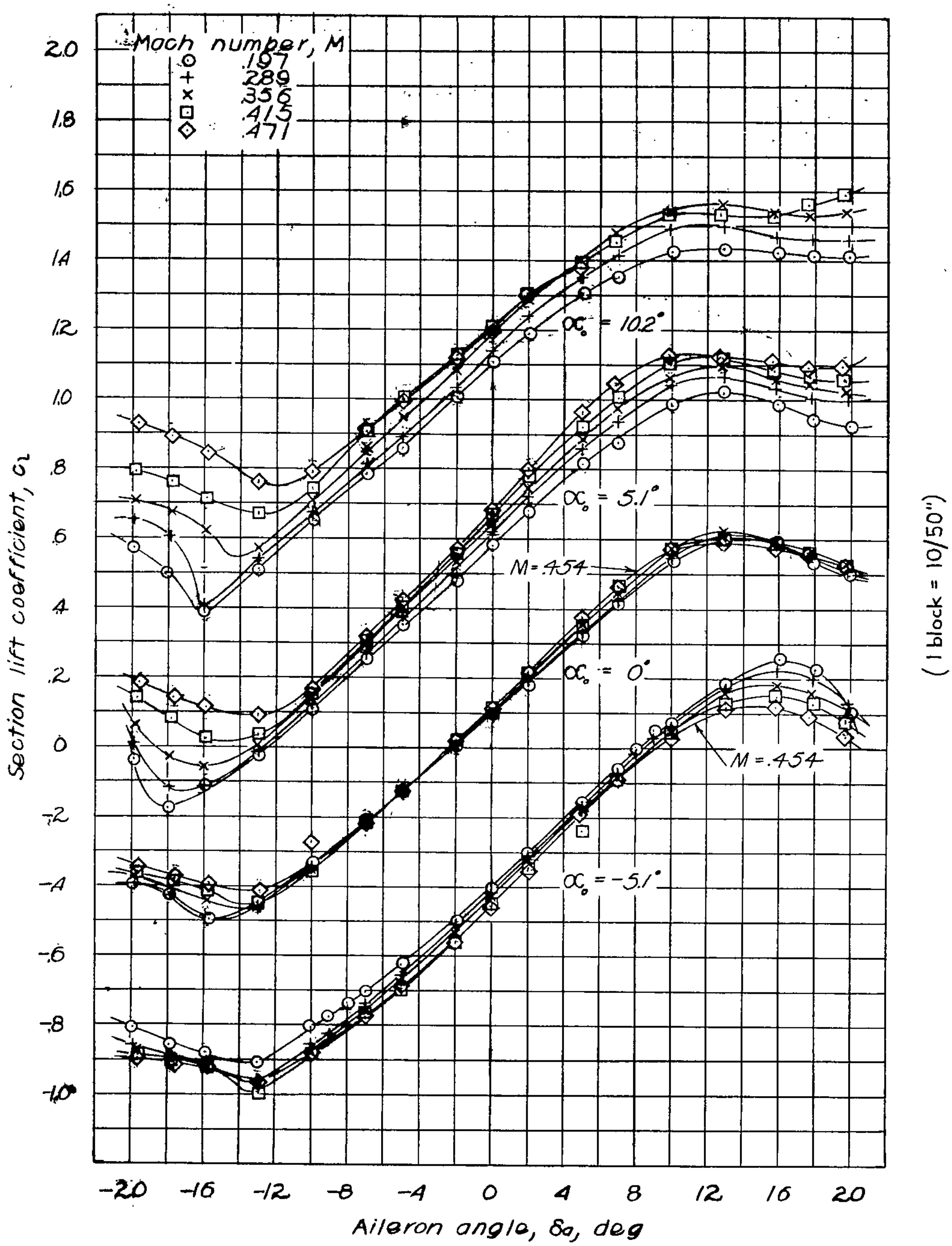

Figure 22.- Variation of section lift coefficient with aileron angle. Nose radii = 0.01c; gap width = 0.0055c.

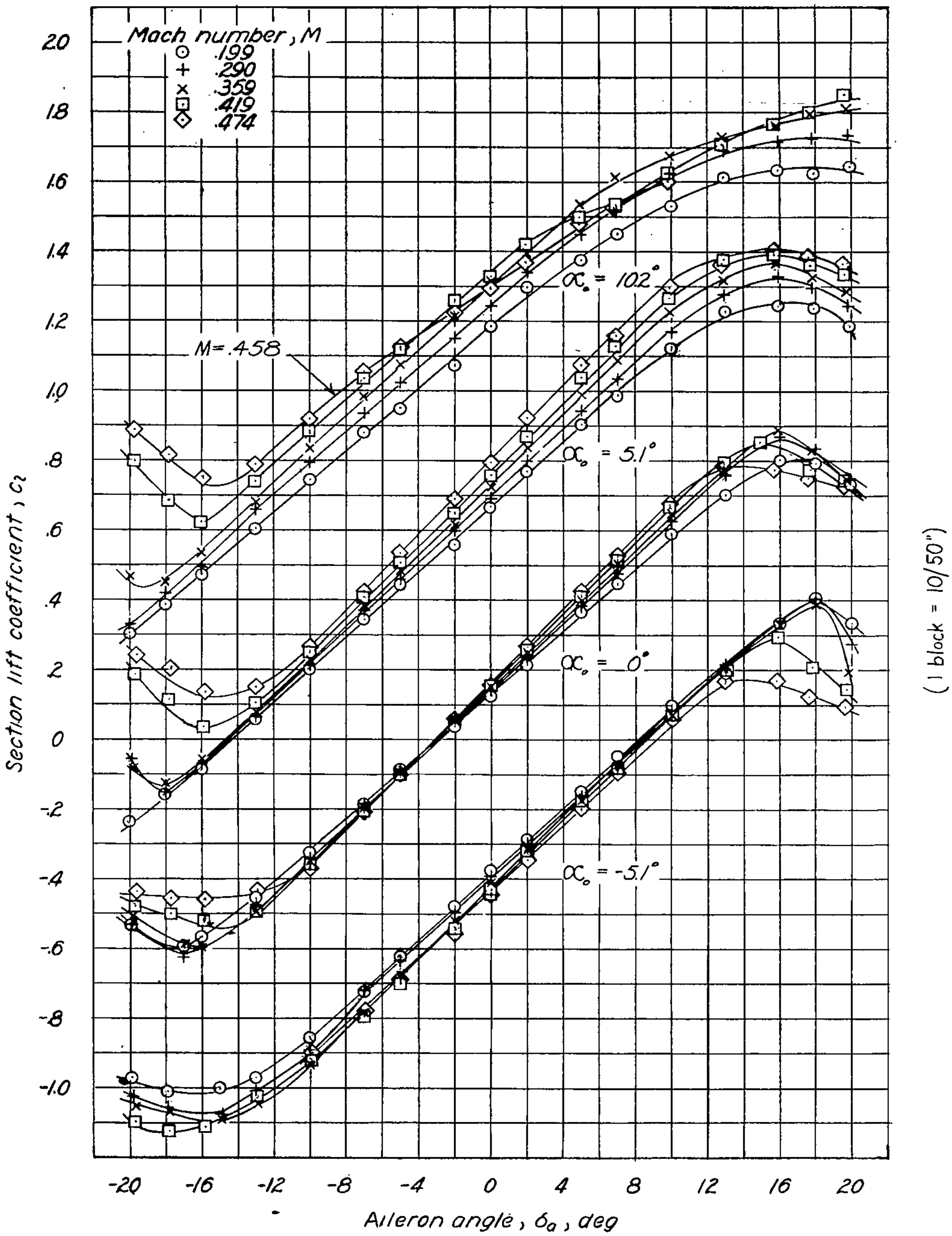

Figure 23.- Variation of section lift coefficient with aileron angle. Nose radii = 0.02c ; gap width = 0.0005c.

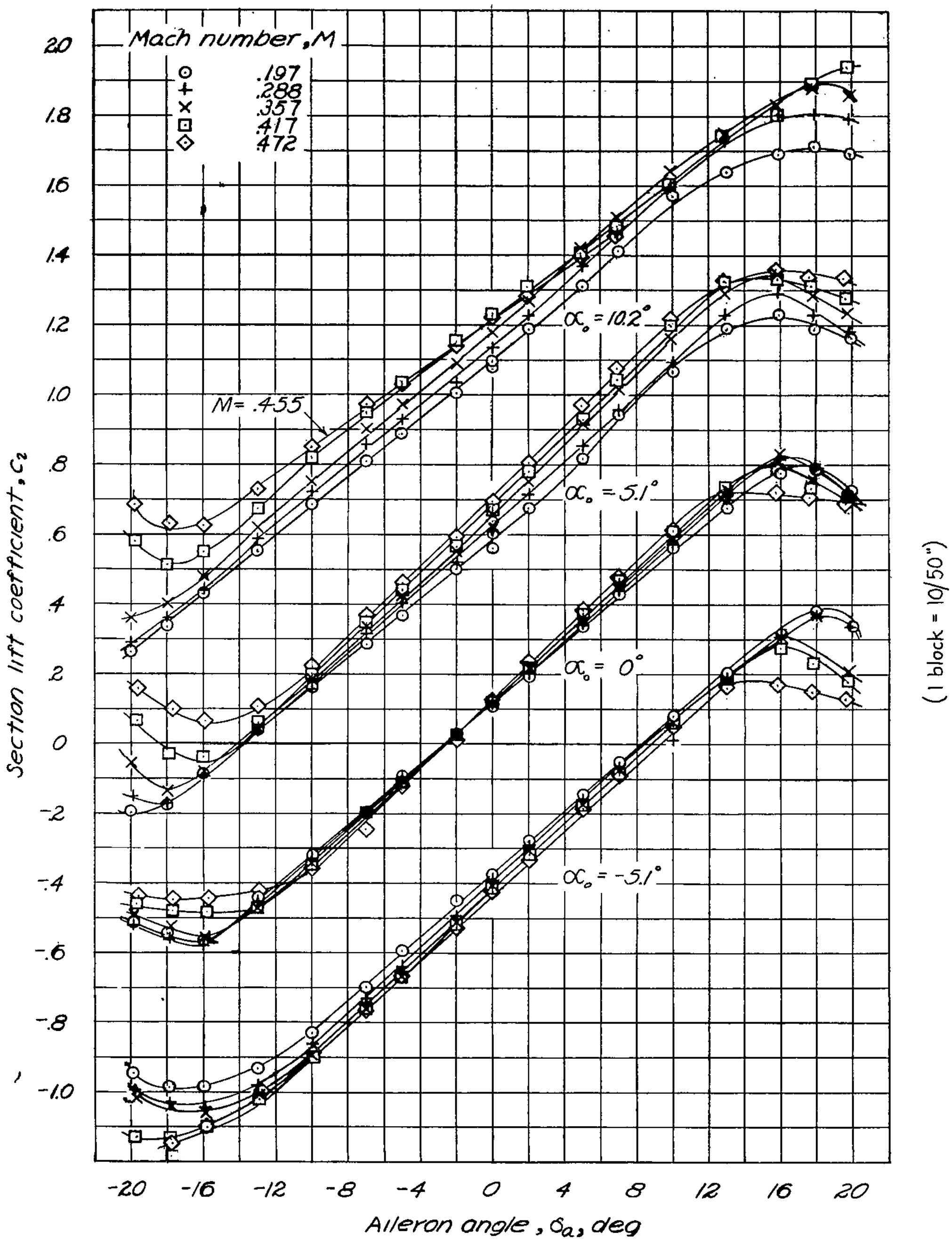

Figure 24.- Variation of section lift coefficient with aileron angle. Nose radii = 0.02c; gap width = 0.0030c.

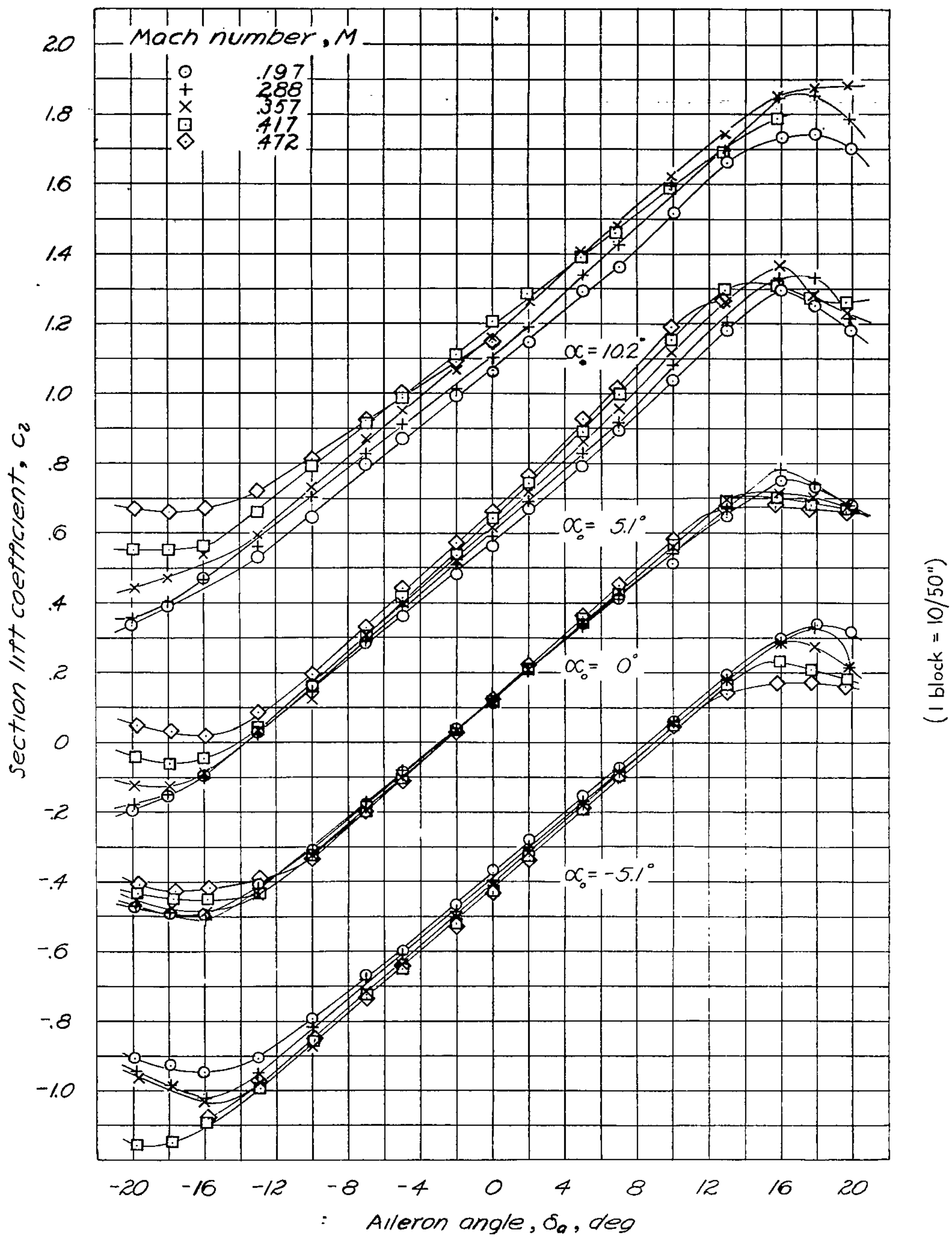

Figure 25.- Variation of section lift coefficient with aileron angle. Nose radii = 0.02c; gap width = 0.0055c.

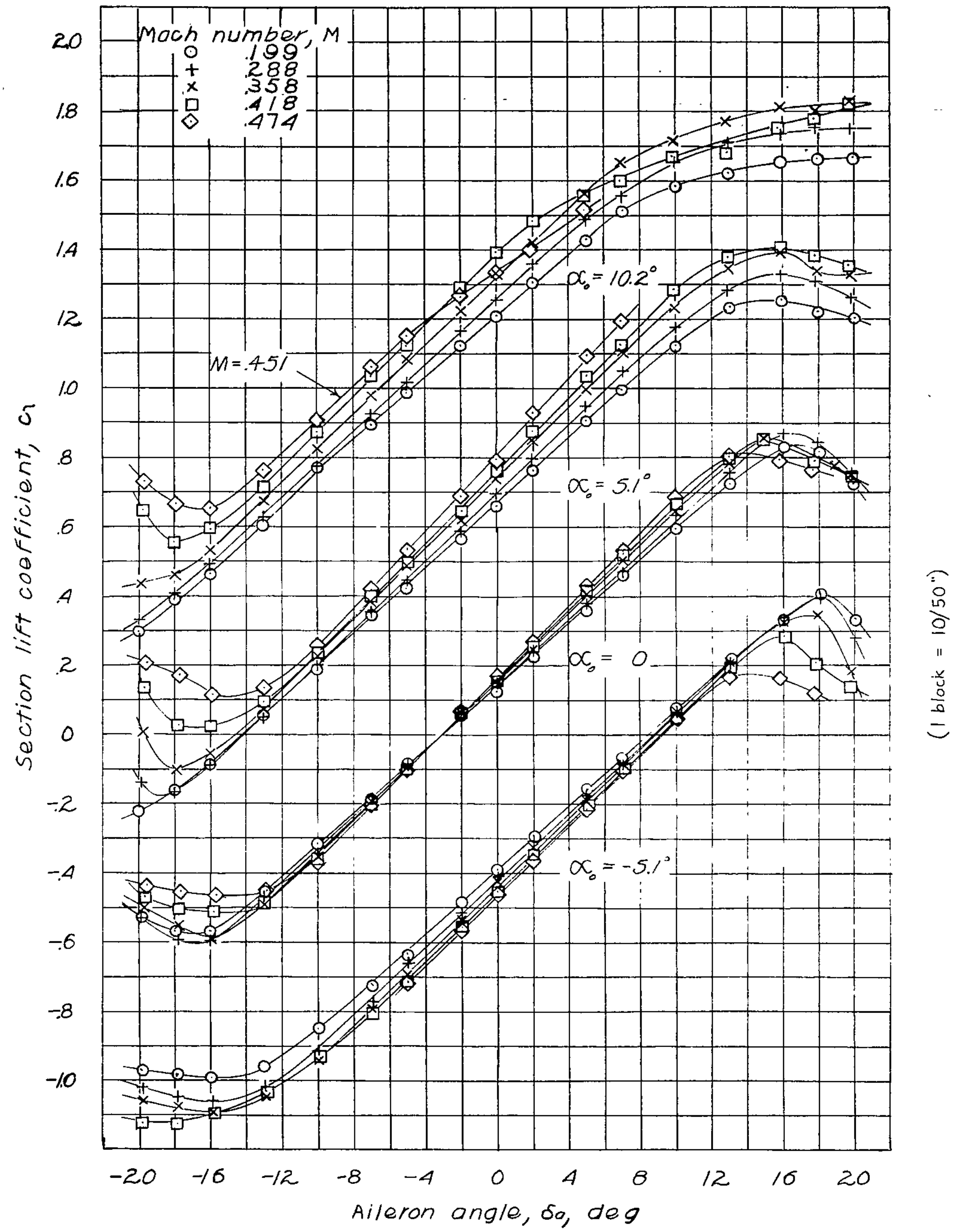

Figure 26.- Variation of section lift coefficient with aileron angle. Nose radii=0.02c; gap width =0.0055c sealed.

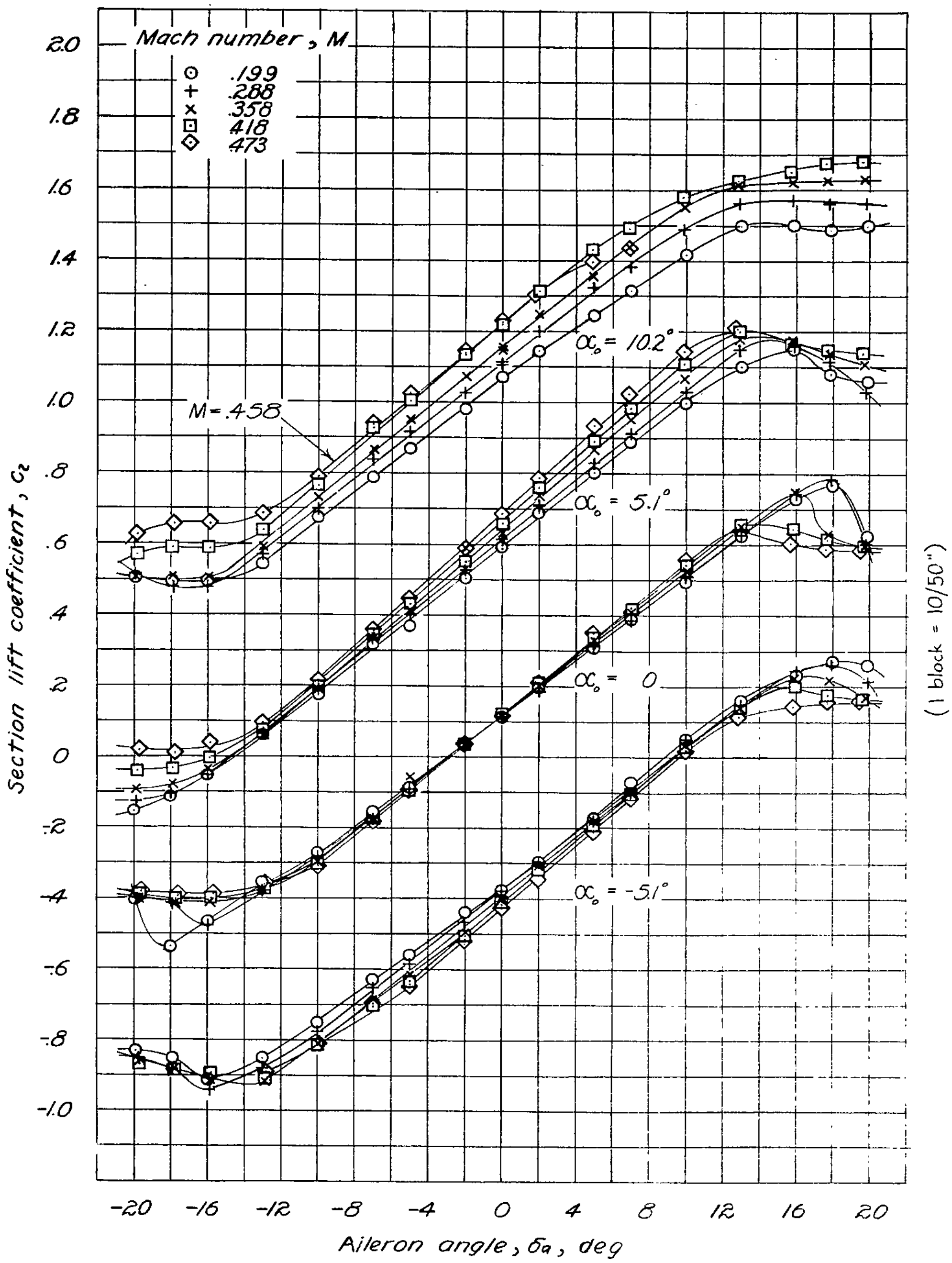

Figure 27.- Variation of section lift coefficient with aileron angle. Nose radii = 0.02c; gap width = 0.0107c.

L-433

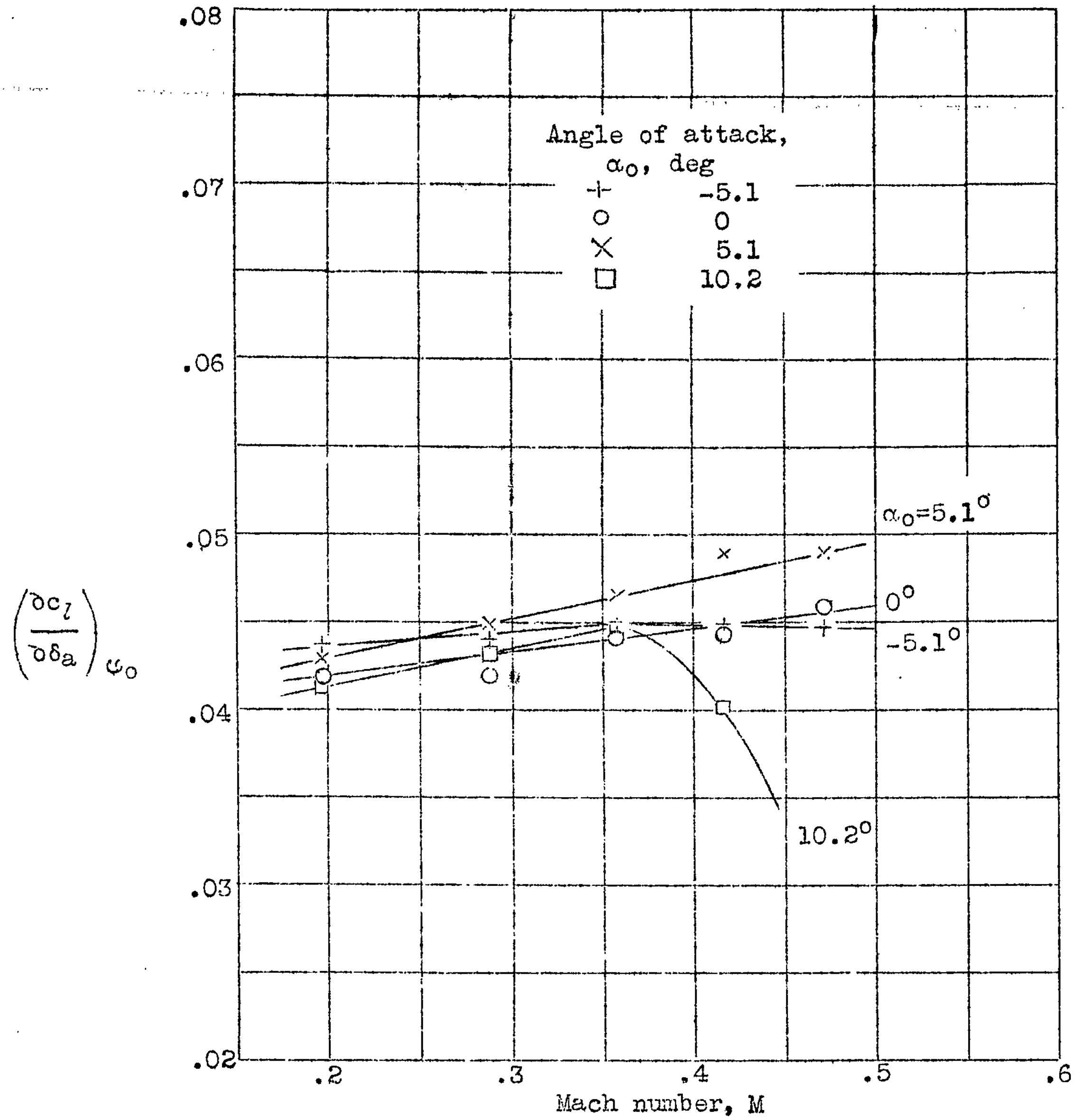

Figure 28.- Effect of a variation of Mach number on the slope of the curve of lift coefficient with aileron angle. Gap width = 0.0055c; nose radii = 0.02c.

L-433

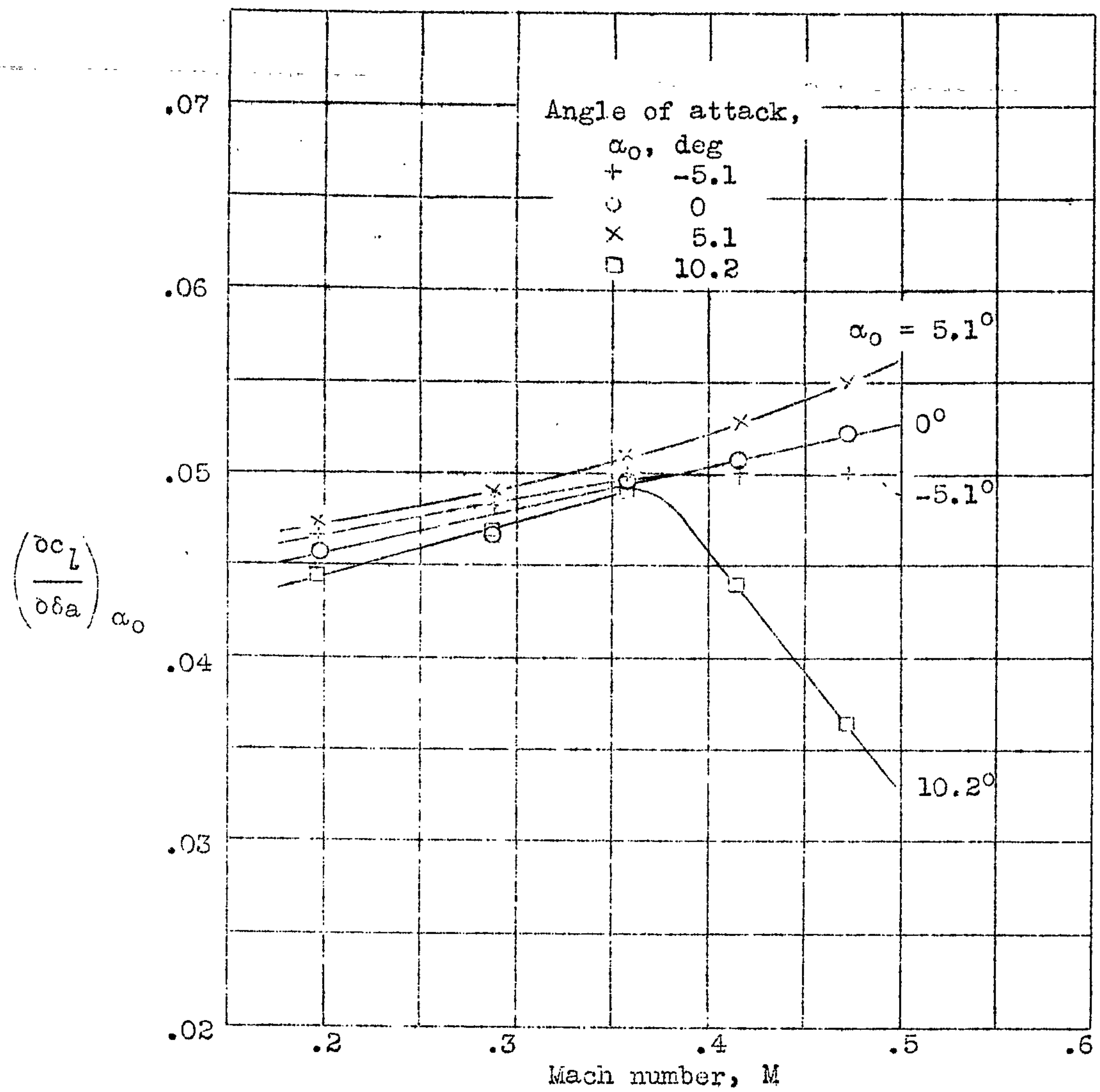

Figure 29.- Effect of a variation of Mach number on the slope of the curve of lift coefficient with aileron angle. Gap width = 0.0055c (sealed); nose radii = 0.02c.

L-433

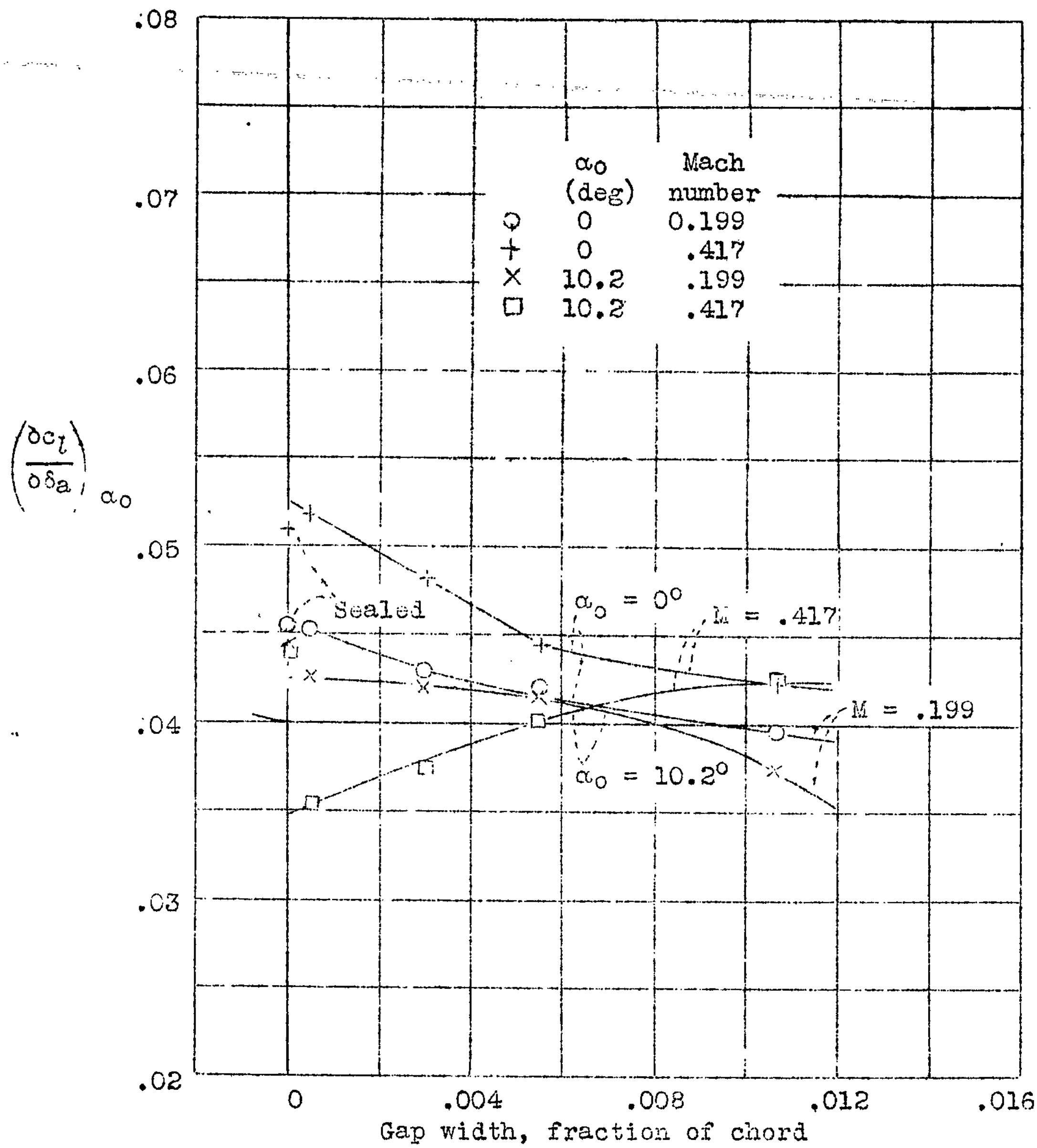

Figure 30.- Effect of a variation of gap width on the slope of the curve of lift coefficient with aileron angle. Nose radii = 0.02c.

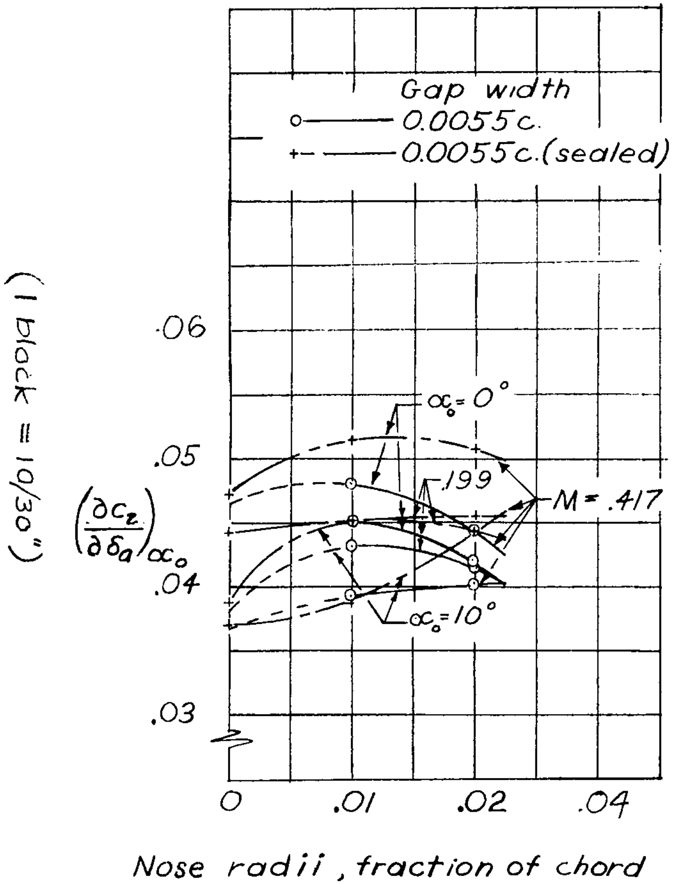

Figure 31.– Effect of nose radii on the slope of the curve of lift coefficient with aileron angle.

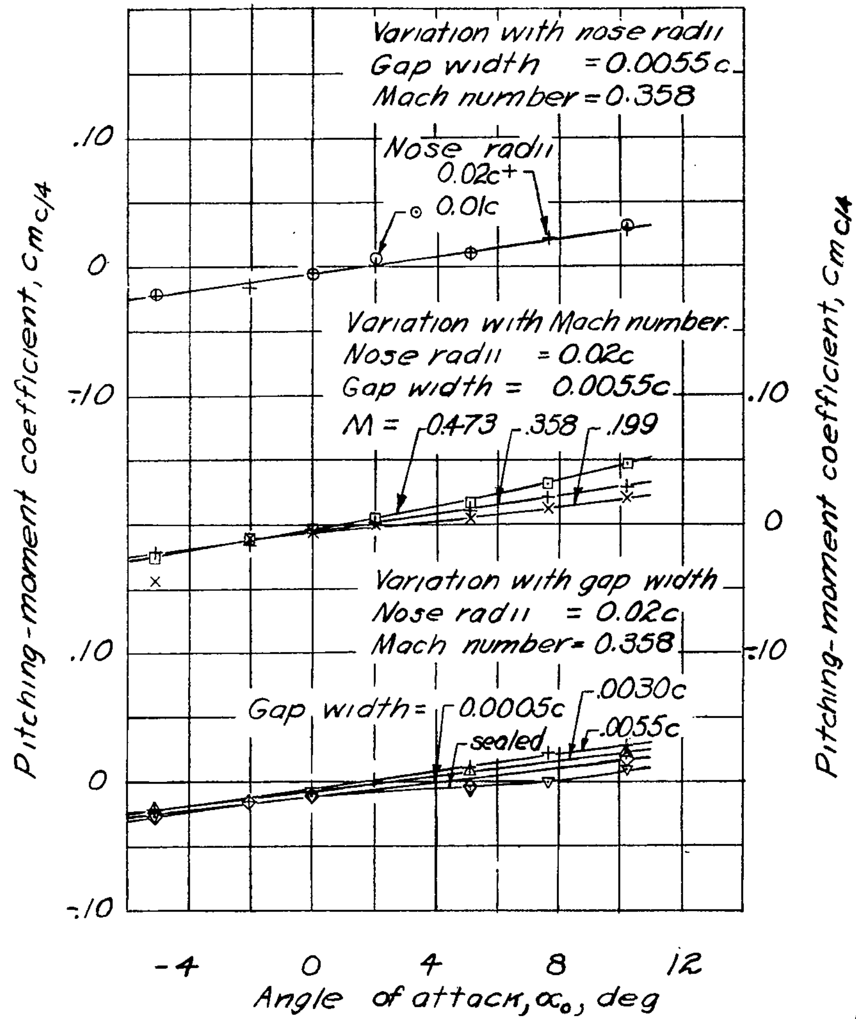

Figure 32.– Variation of section pitching-moment coefficient, obtained by pressure distribution, with angle of attack, for variations of Mach number, nose radii and gap width. $\delta_a = 0°$.